

Physics beyond the Standard Model: experiments at the Gran Sasso Laboratory

A Bettini

DOI: 10.1070/PU2001v044n09ABEH000998

Contents

1. Introduction	931
2. Neutrinos	933
3. Neutrino mixing	935
4. Neutrino masses	937
5. Neutrino oscillations. Contributions of Gran Sasso on atmospheric neutrinos	939
6. Neutrino oscillations. Contributions of Gran Sasso on solar neutrinos	941
7. The next steps	944
8. Neutrinos from CERN	944
9. Atmospheric neutrinos	947
10. Solar neutrinos	948
11. The search for cold dark matter	950
12. Conclusions	953
References	953

Abstract. Experiments in underground laboratories have shown strong evidence of physics beyond the Standard Model. The anomalies observed in electron neutrinos from the sun and muon neutrinos from cosmic rays interacting in the atmosphere can be explained if neutrinos are massive and oscillate. The physics program at the Gran Sasso Laboratory that we are defining will focus on the next phase of neutrino physics with a complementary set of experiments on the muon-neutrino beam from CERN (CNGS project), on solar neutrinos, on atmospheric neutrinos and on neutrinos from supernova explosions. The relevant thermonuclear cross-sections will be measured. The Majorana vs. Dirac nature of electron neutrinos will be explored with the search for neutrinoless double beta decays in different isotopes. Experiments on non-baryonic dark matter are reaching a sensitivity that brings them close to being able to detect neutralinos in certain optimistic theoretical expectations. The program at Gran Sasso for the next years will include a strong effort to increase further the sensitivity by orders of magnitude with different complementary techniques.

1. Introduction

Experiments carried out in underground laboratories are complementary to those done with accelerators as for basic research on the elementary constituents of matter, of their

interactions and symmetries. Searching for natural occurrences of rare phenomena is the only way to reach, even if indirectly, the energy scales that are and will always be out of the reach of accelerators. But these are needed if we want understand the unification of the forces and the quantum aspects of gravity. Underground laboratories provide the very low radioactive background environment necessary in the search for these extremely rare nuclear and subnuclear phenomena. Indeed, we have now for the first time strong hints for physics beyond the Standard Model (SM). The evidence lies in neutrino physics and has been obtained in underground laboratories, mainly Kamioka in Japan and Gran Sasso in Italy.

In January 2001 I gave a colloquium at the Lebedev Institute and a seminar at the ITEP in Moscow. This is a written, and somewhat expanded, version. As in the Lebedev colloquium, I'll address a non-specialist reader. After a brief description of the Gran Sasso Laboratory of the INFN (Istituto Nazionale di Fisica Nucleare, the Italian Agency responsible for nuclear and subnuclear physics) and a historic recollection, I'll present an introduction to new neutrino physics in Sections 2 and 3. In Section 4, after having briefly recalled the status of our knowledge of neutrino masses, I'll describe the contributions of experiments at Gran Sasso. Then I'll describe the results on neutrino oscillations with neutrinos both from the sun and from the atmosphere. I'll then go to the program for the next years, describing future experiments and projects proposed to study further new neutrino physics with a neutrino beam from CERN (CNGS project), using atmospheric and solar neutrinos. Finally, present experiments and proposals in the search for dark matter will be discussed.

Gran Sasso Laboratory is located under the Gran Sasso d'Italia Mountain in central Italy, under a 1400-m rock

A Bettini Dipartimento di Fisica G. Galilei dell'Università di Padova, INFN Gran Sasso National Laboratory and Sezione di Padova, Italy
E-mail: Alessandro.Bettini@lngs.infn.it

Received 28 March 2001

Uspekhi Fizicheskikh Nauk 171 (9) 977–1003 (2001)

Translated by A S Mal'gin; edited by O G Ryazhskaya and S V Semenov

coverage. The rather flat shape of the massif provides uniform coverage at all angles, giving a cosmic rays muon flux attenuation factor of 10^6 . The neutron fluence from the sandstone rock is also particularly low (ten times lower than in the Mont Blanc tunnel, for example).

As shown in Fig. 1, the laboratory consists mainly of three halls about 20 m high, 20 m wide and 100 m long and a number of service and safety tunnels. Access is through the gallery of the freeway that joins the cities of L'Aquila and Teramo on the two sides of the mountain. The narrow tunnel close to the freeway is for cars, while the U-shaped tunnel is for lorries, allowing for easy transportation and installation of large pieces of apparatus. The infrastructure of the laboratory is complete with a number of buildings on the surface near the western entrance of the tunnel, which host offices, laboratories, shops, a library, a canteen, etc.

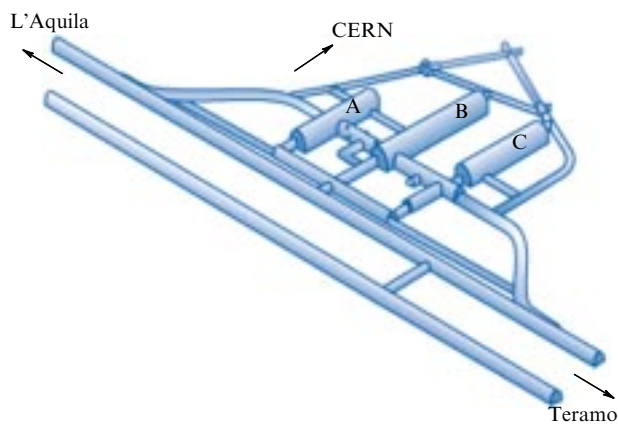


Figure 1. Sketch of the Gran Sasso underground laboratories.

The proposal to build a large, high technology, underground laboratory was advanced in 1979 by A Zichichi, then President of INFN and approved by the Italian Parliament in 1982. Since the original project of Zichichi, the orientation of the halls was towards CERN in order to host detectors to study neutrino oscillations on a beam produced at that laboratory.

Civil engineering work, under the direction of ANAS, the Italian Road Department, started in autumn 1982 and was completed in 1987. By 1989, the first module of a large experiment, MACRO, was taking data. Figure 2 shows a phase of the excavation works in one of the halls, Fig. 3 the hall as completed.

In 1990, the Italian Parliament approved a further law committing ANAS to complete the Gran Sasso Laboratory with two new halls and an independent access tunnel, necessary for guaranteeing high safety standards. If in the 80's immediate action had followed the decisions of Parliament, the new political situation in the 90's has slowed down the realisation of the civil engineering works but, with many obstacles having been overcome, the project now appears finally ready to enter its executive phase.

Experiments at Gran Sasso, which has been in operation a little more than ten years, have already resulted in major discoveries and made important contributions to science [1].

First generation experiments, or at least some of them, are reaching or have reached completion. Upon taking office, I asked the international Scientific Committee of the Laboratory to examine in depth all current experiments in order to

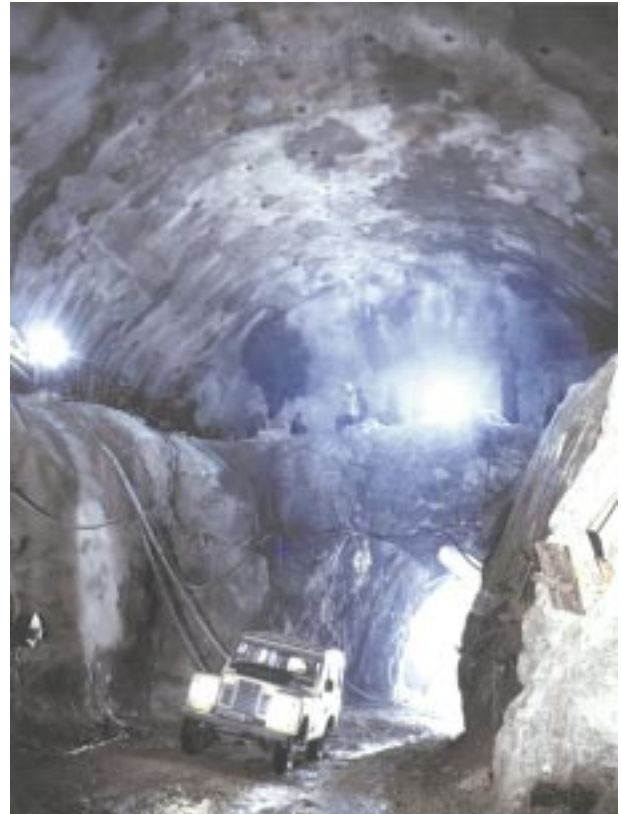


Figure 2. Excavations works in one of the halls.



Figure 3. One of the experimental halls (when it was empty).

determine on scientific grounds how much time would be necessary for each of them to be completed. The experiments had been approved, in fact, without defining how much time they would be occupying space at the underground laboratory.

The review led to the conclusion that in 2001 almost half of the laboratory space will be available to new experiments. The awareness of the availability of space has stimulated the scientific community and a number of very interesting ideas and proposals have been submitted to the Laboratory. It is now clear that first class opportunities are present for the next experimental phase that may, with a bit of fortune, lead to

major discoveries in physics beyond the present theory of elementary particles.

Neutrino physics will be the principal, but not the only, theme of the research program for the next years. As we will see, experiments involving neutrinos that are both naturally produced (from the sun, from the atmosphere and from supernova explosions) and artificially produced (mainly by CERN, but possibly by other sources too) are being created or planned. Some experiments will try to understand the nature of the electron neutrino and search for the Majorana mass, while others will continue with increased sensitivity the search for non baryonic dark matter. Measurements already begun of thermonuclear cross-sections at energies characteristic of the combustion processes of the stars and sun will continue with an improved underground accelerator facility.

2. Neutrinos

We know three different particles, called neutrinos, one for each of the charged leptons. They are more properly called electron neutrino (ν_e), muon neutrino (ν_μ) and tau neutrino (ν_τ) respectively:

$$\begin{pmatrix} e^- \\ \nu_e \end{pmatrix} \begin{pmatrix} \mu^- \\ \nu_\mu \end{pmatrix} \begin{pmatrix} \tau^- \\ \nu_\tau \end{pmatrix}.$$

These are the states produced, via a charged current, by the weak interactions, in pairs like an electron neutrino and a positron, a muon neutrino and a μ^+ , a tau neutrino and a τ^+ . Similarly, when neutrinos are detected via a charged current process, only the charged lepton of its family, never of another family, is observed. We state this by saying that the flavour lepton numbers are conserved. Direct measurements of the masses of each neutrino flavour have given only upper limits and these masses are assumed in the SM to be zero.

Indirect evidence of neutrino masses can be obtained by observing another phenomenon, the quantum oscillation between different neutrino types, as shown by Bruno Pontecorvo in 1957 [2]. He also developed, along with Gribov, the formalism in 1969 [2]. Since then, neutrino oscillations have been systematically searched for in experiments at artificial neutrino sources, accelerators and nuclear reactors, but never reliably established. Even if several experiments did report from time to time positive evidence, they were systematically contradicted by later, more accurate, experiments. Only the latest, controversial LSND result has not been completely contradicted, but neither has it been confirmed. The situation has drastically changed in recent years due to experiments on natural neutrino sources. Experiments on electron neutrinos from the sun and electron and muon neutrinos indirectly produced by cosmic rays in the atmosphere have shown that, most likely, neutrinos oscillate amongst states of definite flavour. This implies that, contrary to the assumptions of the SM, (1) electron, muon, and tau neutrinos are not the stationary states (eigenstates) that we will call ν_1 , ν_2 , and ν_3 , and indicate with m_1 , m_2 and m_3 their masses; (2) at least two of the masses are not zero; (3) flavour lepton numbers are not conserved.

We will discuss now the mixing amongst neutrinos, starting with a simple situation in which only two neutrino flavours, say ν_α and ν_β , exist. These states are linear superpositions of the eigenstates

$$\begin{pmatrix} \nu_\alpha \\ \nu_\beta \end{pmatrix} = \begin{pmatrix} U_{\alpha 1} & U_{\alpha 2} \\ U_{\beta 1} & U_{\beta 2} \end{pmatrix} \begin{pmatrix} \nu_1 \\ \nu_2 \end{pmatrix},$$

where U is the mixing matrix. U being unitary, its elements can be expressed, regarding oscillations, in terms of one real parameter only, usually in the form

$$\begin{pmatrix} \nu_\alpha \\ \nu_\beta \end{pmatrix} = \begin{pmatrix} \cos \theta & \sin \theta \\ -\sin \theta & \cos \theta \end{pmatrix} \begin{pmatrix} \nu_1 \\ \nu_2 \end{pmatrix},$$

where θ is the mixing angle.

Suppose now that a pure ν_α beam, that we assume for the moment to be mono-energetic with energy E is produced. The two eigenstates will then propagate with different velocities and the ν_α and ν_β components of the beam will periodically vary (neutrino oscillation). A simple calculation shows that the probability of detecting ν_β in an initially pure ν_α beam at the flight distance L is

$$P_{\nu_\alpha \rightarrow \nu_\beta} = \sin^2 2\theta \sin^2 \left(1.27 \Delta m^2 [\text{eV}^2] \frac{L [\text{km}]}{E [\text{GeV}]} \right). \quad (1)$$

The probability of observing ν_β 's initially increases from zero, reaches a maximum and then decreases, in a periodic phenomenon called oscillation. The period is inversely proportional to $\Delta m^2 = m_2^2 - m_1^2$, the difference between the squares of the masses of the two eigenstates. Notice that the oscillation probability depends only on the absolute value of the square mass difference and not on its sign. The first oscillation maximum takes place at

$$\frac{L [\text{km}]}{E [\text{GeV}]} = \frac{\pi}{2 \times 1.27} \frac{1}{\Delta m^2} \approx \frac{1}{\Delta m^2 [\text{eV}^2]}. \quad (2)$$

The second parameter in Eqn (2), $\sin^2 2\theta$, gives the amplitude of the oscillation probability. If $\theta = \pi/4$, the maximum oscillation probability is 100% (maximum mixing).

The results of the oscillation searches are reported in the parameters plane Δm^2 vs. $\sin^2 2\theta$. All the *a priori* possible situations are described by mixing angle values ranging in the first octant, $0 \leq \theta \leq \pi/4$. Notice that this is correct only if the neutrino flavour is two (and not three) and if they fly in a vacuum.

Expression (1), which gives the probability of the appearance of a new flavour, is relevant for appearance experiments that try to detect ν_β 's. Obviously, the probability of observing the original flavour (disappearance experiments) is

$$P_{\nu_\alpha \rightarrow \nu_\alpha} = 1 - \sin^2 2\theta \sin^2 \left(1.27 \Delta m^2 [\text{eV}^2] \frac{L [\text{km}]}{E [\text{GeV}]} \right). \quad (3)$$

In practice, neutrino sources, both natural and artificial, do not produce a mono-energetic neutrino flux, neither detectors measure neutrino energy with infinite resolution. Let us then consider the expression (3) of the disappearance probability if E is not well defined. We will assume maximum mixing. For each energy, initially the probability of observing the original flavour is one. When L/E increases (the beam propagates) the probability decreases, again for all components. Then, one after the other, the probabilities of the components reach the minimum. Proceeding further, the probability of some components will increase while for others it will decrease, so that after the first minimum, the finite energy resolution averages out the different contributions, which are between 0 and 1, to 0.5. As shown in Fig. 4a the result is that the probability of observing the original flavour as a function of the distance from the source passes

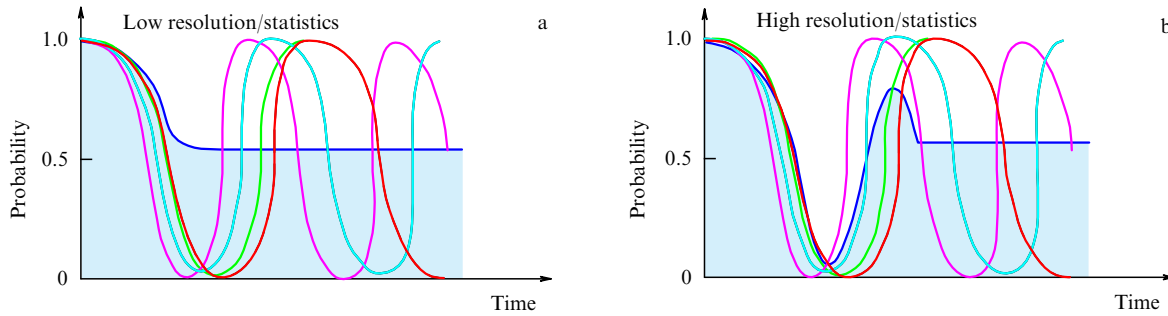


Figure 4. Oscillation probability for non mono-energetic neutrinos.

from the original 100% to 50% at the first oscillation minimum (first for the average energy).

The position (time) of the downward step in Fig. 4 gives Δm^2 , its height $\sin^2 2\theta$. It is indeed possible to observe a full oscillation pattern by designing an experiment with sufficient resolution in the crucial L/E parameter and with sufficient statistics, as shown in Fig. 4b (see, for example, the MONOLITH proposal which follows).

Lepton mixing is formally identical to quark mixing, but is very different quantitatively. In the quark case (the first two families) θ is the Cabibbo angle and is small, while in the lepton case, as we will see, the mixing appears to be very large, probably close to the maximum. To gain insight, let us consider explicitly this case. We have

$$\begin{pmatrix} \nu_\alpha \\ \nu_\beta \end{pmatrix} = \begin{pmatrix} \frac{1}{\sqrt{2}} & \frac{1}{\sqrt{2}} \\ -\frac{1}{\sqrt{2}} & \frac{1}{\sqrt{2}} \end{pmatrix} \begin{pmatrix} \nu_1 \\ \nu_2 \end{pmatrix}$$

or

$$\nu_\alpha = \frac{1}{\sqrt{2}}(\nu_1 + \nu_2), \quad \nu_\beta = \frac{1}{\sqrt{2}}(-\nu_1 + \nu_2).$$

In the quark case, quarks of definite flavour are very close to an eigenstate, while neutrinos with definite flavour are very different from the eigenstates.

It is interesting to discuss a mechanical analogy of neutrino oscillations. Consider two identical pendulums of length L and mass m . Each of them, if initially excited, will vibrate in a harmonic motion, with square (proper) angular frequency $\omega^2 = g/L$. If we connect them with a spring, constant k , the two pendulums are coupled. This system has two stationary states (or modes): (1) the two pendulums vibrate in phase with the same amplitude; the square eigenfrequency of this mode is $\omega_1^2 = g/L$ (the spring remains in its natural length and does not exert any force); (2) the two pendulums vibrate, again in phase but with equal and opposite amplitudes; the square eigenfrequency is $\omega_2^2 = g/L + 2k/m$. These states are analogous to ν_1 and ν_2 and the eigenfrequencies are analogous to the masses.

The states analogous to ν_α and ν_β are those in which one or the other pendulum vibrates. Let us then bring the pendulum α out of equilibrium and let it go. We observe that the other pendulum, β , will start to vibrate with an initially small but gradually increasing amplitude, reaching a maximum when all the energy has been transferred from α to β . Then the process will reverse itself and the energy will go back to α . Energy, analogous to probability, oscillates back and

forth between the two pendulums with the angular frequency $\omega_2 - \omega_1$. Indeed the motion of α (for example) is

$$\begin{aligned} \frac{1}{\sqrt{2}}(\cos \omega_1 t + \cos \omega_2 t) \\ = \frac{1}{\sqrt{2}} \cos\left(\frac{\omega_2 - \omega_1}{2} t\right) \cos\left(\frac{\omega_2 + \omega_1}{2} t\right) \end{aligned}$$

and its energy is proportional to the square of the amplitude, i.e., to $\cos^2[(\omega_2 - \omega_1)/2 t]$ whose frequency is $\omega_2 - \omega_1$. Notice that the measurement of the energy oscillation frequency determines the absolute value of the difference between the two eigenfrequencies and not its sign.

It is easy to see that if the two pendulums are not identical, that is, if they have different lengths, the same phenomenon will occur, but with an important difference. Starting again with α excited, its energy will pass to β , with the same period as before, but only partially. The fraction of energy transfer decreases as the difference between the lengths of the pendulums increases. Maximum mixing occurs when the two pendulums are identical or, better, when, taken alone, have the same period.

Let us consider also a slightly different mechanical analogue, that I'll refer to later. In place of the two pendulums, let us consider two oscillators made of a small sphere at one end of an elastic bar. The other ends of the bars are fixed. The two elastic oscillators are coupled like the pendulums. If the two are identical, the mixing is maximised, while if they have different masses, the mixing is less than the maximum. Again, maximum mixing corresponds to a symmetric system.

If an electron-neutrino (or antineutrino) beam propagates into matter (in the sun, the earth or a supernova) another mechanism may cause flavour conversion, the so-called MSW effect [3]. Electron neutrinos (and antineutrinos) interact with electrons via charged current weak interactions, and coherent forward scattering, a phenomenon exactly similar to the forward scattering of light in matter at the origin of the refractive index, occurs. Similarly, the electron-neutrino wave acquires a refractive index different than in a vacuum, or, equivalently a different effective mass.

The effect is limited to electron neutrinos because the other neutrino flavours interact via neutral current only and the effects of negative (electrons) and positive (nuclei) compensate. The effect is related to the electron density (ρ) times the neutrino energy (E). In appropriate conditions a level crossing, or resonance if one prefers, phenomenon takes place: at a critical ρE value the effective electron-neutrino 'mass' becomes equal to that of a different flavour. Electron neutrinos will convert into neutrinos of that flavour, or vice

versa, while crossing a variable density medium when they reach this critical value.

Considering for the sake of simplicity a medium of uniform density, the oscillation probability can be written in the form

$$P_{\nu_\alpha \rightarrow \nu_\beta} = \sin^2 2\theta_m \sin^2 \left(1.27 \Delta m_m^2 [\text{eV}^2] \frac{L [\text{km}]}{E [\text{GeV}]} \right), \quad (4)$$

where we have introduced the effective mixing angle θ_m and the effective square mass difference Δm_m^2 to take into account the matter effect

$$\begin{aligned} \Delta m_m^2 &= \sqrt{(\Delta m^2 \cos 2\theta - A)^2 + (\Delta m^2 \sin 2\theta)^2}, \\ \sin 2\theta_m &= \frac{\Delta m^2}{\Delta m_m^2} \sin 2\theta, \end{aligned} \quad (4')$$

$$A = 2\sqrt{2} G_F N_e E \Rightarrow A [\text{eV}^2] = 7.6 \times 10^{-5} \rho [\text{g cm}^{-3}] E [\text{GeV}],$$

where G_F is the Fermi constant and N_e is the electron density. Resonance exists only if Δm^2 is positive, when the product ρE is such that $A = \Delta m^2 \cos 2\theta$. Under these conditions $\sin 2\theta_m = 1$, i.e., the mixing is at an effective maximum for any value of $\sin 2\theta$. Δm_m^2 , that is always smaller than Δm^2 , and is at a minimum at resonance $\Delta m_m^2 = \Delta m^2 \sin 2\theta$. There is no resonance for $\Delta m^2 < 0$. Notice that the effect is different for electron neutrinos and antineutrinos.

Notice also that in the presence of matter the full range $0 \leq \theta < \pi/2$ is relevant, not only the first octant as in a vacuum.

To get an idea of the orders of magnitude, consider the electron neutrinos crossing the sun. For a typical density of $10 - 100 \text{ g cm}^{-3}$ and neutrino energy of 1 MeV, resonance can happen if $\Delta m^2 \approx 10^{-5} - 10^{-6} \text{ eV}^2$.

Let us consider again the system of two coupled elastic oscillators. If they have different masses the mixing is not at a maximum. But by sinking the heavier one in a liquid of the appropriate density we can bring its mass closer to that of the other, thus increasing the ‘effective’ mixing. For a critical density of the liquid we can make the two masses ‘effectively’ equal. Clearly, we cannot obtain maximum mixing (level crossing) by sinking the lighter pendulum in a liquid.

3. Neutrino mixing

We have experimental evidence of neutrinos of three different flavours; we also know from the width and height of the Z_0 peak that there are exactly three. We cannot exclude that neutrino states not coupled to Z_0 exist, even at low masses; they are called sterile neutrinos, but their presence is not requested by any confirmed experiment. The simplest possibility is to assume that, similarly to quarks, neutrino states with definite flavour, that is, those produced by weak interactions and detected by our instruments, are linear combinations of the eigenstates

$$\begin{pmatrix} \nu_e \\ \nu_\mu \\ \nu_\tau \end{pmatrix} = \begin{pmatrix} U_{e1} & U_{e2} & U_{e3} \\ U_{\mu1} & U_{\mu2} & U_{\mu3} \\ U_{\tau1} & U_{\tau2} & U_{\tau3} \end{pmatrix} \begin{pmatrix} \nu_1 \\ \nu_2 \\ \nu_3 \end{pmatrix}. \quad (5)$$

The mixing matrix being unitary, its elements can be expressed in terms of four independent real parameters, usually given as three ‘mixing angles’ and a phase factor.

The phase factor gives CP violating effects in the lepton sector, which is extremely important but, unfortunately, still very far from being experimentally accessible. As a consequence, we will, for simplicity, forget the phase factor and consider only real matrix elements. We will adopt for the mixing angles the most commonly used notation θ_{12} , θ_{13} and θ_{23} , even if it is somewhat misleading, as θ_{12} is not the mixing angle between ν_1 and ν_2 , etc. Two further phases, α and β , irrelevant for oscillations, are present if the neutrinos are Majorana particles.

In terms of the mixing angles, the mixing matrix can be written (denoting with c_{12} the cosine of θ_{12} , s_{12} its sine, etc.) as the product of three matrices

$$U = \begin{pmatrix} 1 & 0 & 0 \\ 0 & c_{23} & s_{23} \\ 0 & -s_{23} & c_{23} \end{pmatrix} \begin{pmatrix} c_{13} & 0 & s_{13} \\ 0 & 1 & 0 \\ -s_{13} & 0 & c_{13} \end{pmatrix} \begin{pmatrix} c_{12} & -s_{12} & 0 \\ s_{12} & c_{12} & 0 \\ 0 & 0 & 1 \end{pmatrix}. \quad (6)$$

The situation is now much more complex than in the case of only two neutrino states. Two different oscillations take place (in the case of neutrinos) with different frequencies, meaning at different times. The expressions for the probability of observing a state of definite flavour are much more complicated than Eqn (1). Just to give an example, an approximate expression of the probability of observing an electron neutrino in an initially (monochromatic) muon-neutrino beam propagating in a vacuum is

$$P_{\nu_\mu \rightarrow \nu_e} = \sin^2(\theta_{23}) \sin^2(2\theta_{13}) \sin^2 \left(1.27 \Delta m^2 [\text{eV}^2] \frac{L [\text{km}]}{E [\text{GeV}]} \right). \quad (7)$$

Although this is not the complete formula, it is a good approximation of flight times relevant to the first oscillation when the second slower one has not yet started. Notice that the probability amplitude now depends on the two mixing angles. Notice also that the probability is different if one of the angles, θ_{23} , is in the first or second octant. Considering all the cases, one sees that the full range $0 \leq \theta_{12}, \theta_{13}, \theta_{23} \leq \pi/2$ must be considered, and not $0 - \pi/4$ as is still frequently, but wrongly, done. The variable $\sin^2 2\theta$ should not be used: better variables are $\sin^2 \theta$ or $\tan^2 \theta$ [4] or just θ . In practice, I’ll sometimes be forced to use $\sin^2 2\theta$ in the following, when quoting results presented in this form, but only in cases safe from error.

The search for neutrino oscillations has been going on for decades with artificial neutrino beams from accelerators (mainly muon neutrinos) and reactors (electron antineutrinos) but so far no reliable experiment has reported a positive result confirmed by a different experiment. This can be understood if the square mass differences are so small that the oscillation times, or the flight paths required to observe the oscillations, are very large, much larger than the usual lengths, order of 1 km, of the neutrino beams¹.

On the other hand, deficits in the fluxes of electron neutrinos from the sun and muon neutrinos from atmosphere have been observed with increasing reliability and precision. The simplest interpretation of both anomalies is that they are due to two different oscillation phenomena, both at L/E values much larger than those available at accelerators thus far (K2K experiment, see later).

¹ The length of the beam is here the distance between the neutrino source and the detector.

We will now present a short summary of our present understanding here and give the details later.

Electron neutrinos are produced by thermonuclear processes in the core of the sun; when the flux of neutrinos of this flavour is measured on earth, substantially lower values than expected are found. This, together with other more detailed findings, as we will see, can be explained only if neutrinos behave in a non-standard way, the simplest hypothesis being oscillation (including the MSW effect). Solar neutrino data do not point to a unique solution but are compatible with a few: three of them are mainly MSW transitions and are called ‘small mixing angle’ (SMA; $\delta m^2 \approx 10^{-5}$ eV², $\tan^2 \theta_{12} \approx 10^{-3} - 10^{-4}$), ‘large mixing angle’ (LMA; $\delta m^2 \approx 10^{-4} - 10^{-5}$ eV², $\tan^2 \theta_{12} \approx 0.5 - 1$), and LOW ($\delta m^2 \approx 10^{-7} - 10^{-8}$ eV²; $\tan^2 \theta_{12} \approx 0.5 - 1$), while the fourth is applicable to oscillations in a vacuum ($\delta m^2 \approx 10^{-9} - 10^{-12}$ eV², $\tan^2 \theta_{12} \approx 1$). Solar neutrinos give information for the first line of the mixing matrix (5), or, in other words, for the last of the three factors in Eqn (6). All solutions indicate a small value of $|U_{e3}|^2$ (with a large uncertainty), and all but one (SMA), as we have just seen, are close or equal to ‘maximum mixing’, meaning here that $|U_{e1}|^2 \approx |U_{e2}|^2 \approx 1/2$ (within a large uncertainty) or θ_{12} close to $\pi/4$.

The second anomaly has been convincingly observed by the Super-Kamiokande and confirmed by MACRO in ‘atmospheric’ neutrinos. Atmospheric neutrinos give information for the elements of the third column of the mixing matrix or for the first factor in its expression (6). Neutrinos in the two electron and muon flavours are indirectly produced by cosmic rays in the atmosphere (in a ratio roughly 1:2). Neutrinos reach a detector from different directions from zenith to nadir; the corresponding flight lengths range from 10 km to 12000 km. While the measured electron-neutrino flux is in accordance with expectations at all flight lengths, that of muon-neutrinos is in accordance with expectations at shorter lengths, but half of that expected at larger lengths. The simplest interpretation is that we are observing a second oscillation phenomenon, namely $\nu_\mu \leftrightarrow \nu_\tau$. The square mass difference, as measured by the Super-Kamiokande, is

$$1.5 \times 10^{-3} \text{ eV}^2 < \Delta m^2 < 5 \times 10^{-3} \text{ eV}^2.$$

Mixing may be at a maximum, meaning now that $|U_{\mu 2}|^2 \approx |U_{\mu 3}|^2 \approx 1/2$ (with a sizeable uncertainty) or θ_{23} is close to $\pi/4$. The non-observation of the $\nu_\mu \leftrightarrow \nu_e$ component implies again that the $|U_{e3}|$ matrix element is small (with sizeable uncertainty).

A very important contribution has been made by the CHOOZ [5] experiment, which measured the flux of electron antineutrinos at a distance of 1 km from the source (two power reactors). It is a disappearance experiment that gives information on $|U_{e3}|$ or, in other words, on the second matrix in Eqn (6). The L/E values of this experiment are to the right of the first oscillation maximum of the atmospheric oscillation, maximising the sensitivity. Having found no evidence for oscillations, the experiment gives the stringent limit $\sin^2 2\theta_{13} \leq 0.1$, which implies either $\theta_{13} \leq 9^\circ$ or $\theta_{13} \geq 81^\circ$. The second possibility is ruled out by solar data and we have the limit $|U_{e3}|^2 < 0.03$.

Before concluding this section, let us assume that in both solar and atmospheric anomalies the mixing is at a maximum, i.e. that $\theta_{12} = \pi/4$, $\theta_{23} = \pi/4$ and that $\theta_{13} = 0$ ($|U_{e3}|^2 = 0$). This so-called ‘bi-maximal mixing’ is compatible with all data but is only one of many different possibilities. The mixing

matrix would be

$$U = \begin{pmatrix} \frac{1}{\sqrt{2}} & -\frac{1}{\sqrt{2}} & 0 \\ \frac{1}{2} & \frac{1}{2} & -\frac{1}{\sqrt{2}} \\ \frac{1}{2} & \frac{1}{2} & \frac{1}{\sqrt{2}} \end{pmatrix}. \quad (8)$$

A mechanical analogue in this case is the following [6]. Consider three pendulums, all with the same length and hence with the same period. Two of them, those at the sides (call them μ and τ), have equal masses (m), while that at the centre (call it e) is twice their mass ($2m$). The central pendulum (e) is coupled to each of those on the sides by identical springs with a small elastic constant k . The two side pendulums are also coupled by a spring of larger constant K . The system is shown in Fig. 5.

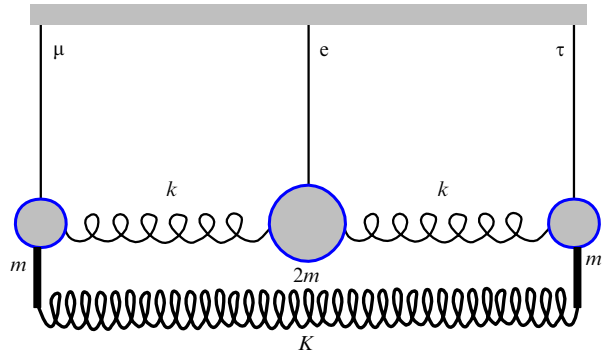


Figure 5. Triple coupled pendulums with ‘bi-maximal’ mixing.

Let us now bring pendulum e out of equilibrium and let it go. The other two, μ and τ , act in these conditions as a single pendulum with twice the mass of each, hence with the same mass as e . The behaviour is thus similar to that of the symmetric double pendulum. The energy oscillates from e to the pair μ and τ , which move as a rigid body with a period proportional to $\sqrt{m/k}$. This is ‘solar’ oscillation, where electron neutrinos disappear and a state that is a quantum superposition of muon and tau neutrinos appears, where mixing is bi-maximal.

If we start with the pendulum μ excited, its energy will initially transfer to pendulum τ and back with a period proportional to $\sqrt{m/K}$. Later, at times of the order of $\sqrt{m/k}$, pendulum e will start to move. This is atmospheric oscillation.

In conclusion, we see that bi-maximal mixing corresponds to a mechanical system that is symmetric. If neutrino mixing were indeed bi-maximal, this would point, I believe, to a deep symmetry of nature.

The small mixing angle (SMA) constitutes the other possible solution to the solar anomaly. Taking the extreme values $\theta_{12} = 0$, $\theta_{13} = 0$, and $\theta_{23} = \pi/4$, the mixing matrix would be

$$U = \begin{pmatrix} 1 & 0 & 0 \\ 0 & \frac{1}{\sqrt{2}} & -\frac{1}{\sqrt{2}} \\ 0 & \frac{1}{\sqrt{2}} & \frac{1}{\sqrt{2}} \end{pmatrix}. \quad (9)$$

4. Neutrino masses

From the evidence briefly reported in the previous section, we can assume that the neutrino mass spectrum consists of two nearby levels, m_1 and m_2 , and a third, more distant one, m_3 . The smaller mass difference $\delta m^2 = m_2^2 - m_1^2$ is responsible for the solar anomaly, the larger one $\Delta m^2 = m_3^2 - m_2^2 \approx m_3^2 - m_1^2$ for the atmospheric anomaly. In other words, the neutrino mass spectrum is composed of a doublet of states very close together and a third, more separate state. The last is a superposition of ν_μ and ν_τ of almost one to one, with possibly a small ν_e component.

As neutrino oscillations depend on the absolute value of the difference between the squares of the masses, we do not know whether the third state is higher ($\Delta m^2 > 0$, called ‘normal’ spectrum) or lower ($\Delta m^2 < 0$, called ‘inverted’ spectrum) than the doublet.

Neither do we know the absolute scale of the masses. There are two extreme possibilities (and the entire range in-between):

(1) The ‘degenerate’ case, when the three masses are almost equal, and are much larger than the difference among them. Due to the experimental limit on the ‘electron-neutrino mass’, the masses cannot be larger than a few electron-volts (see later);

(2) The hierarchical case, when two of the masses are of the order of the square roots of the two square mass differences.

Notice that mass is a property of the stationary states (the eigenstates) and talking of ν_e , ν_μ or ν_τ mass (as we have just done) is improper and in some cases misleading. What is meant depends in fact on what one measures and how one measures it (or limits it).

Consider as an important example the limits on the ‘electron neutrino mass’ $\langle m_{\nu_e} \rangle$ that are obtained by measuring the electron energy spectrum in the tritium beta decay. Near the end point the slope is zero, if the neutrinos have no mass. If the neutrinos are massive, the maximum electron energy decreases (because the smallest mass, say $m_1 \neq 0$) and the spectrum ends with a step of vertical slope. Two further steps are present near the end point, corresponding to the non zero values of m_2 and m_3 . The heights of the steps are closely related to $|U_{e1}|^2$, $|U_{e2}|^2$ and $|U_{e3}|^2$. In principle, with infinite resolution and statistics the three masses and three mixing parameters can be extracted from the spectrum. In practice, the mass differences are so small that they cannot be resolved and one measures an average effect, that, if the resolution function is much wider than the difference amongst the steps, is [6]

$$\langle m_{\nu_e}^2 \rangle = |U_{e1}|^2 m_1^2 + |U_{e2}|^2 m_2^2 + |U_{e3}|^2 m_3^2. \quad (10)$$

Presently two experiments give the upper limit $\langle m_{\nu_e} \rangle < 3$ eV [7].

Let us recall now that in the SM the lepton states are represented by two-component left spinors, i.e. by $\psi_L = (1 + \gamma_5)\psi$, where ψ is a 4-component Dirac spinor. Under CPT it transforms in its charge conjugate right spinor representing the antiparticle, say ψ_R^C . Particles and antiparticles have all their charges opposite and must be different. Neutrinos do not have any charge, apart from the lepton number. If this is not a good quantum number, then the neutrinos and the antineutrinos may be the same particle, or $\nu_e^C = \nu_e$. The neutrinos are then (pure) Majorana particles

and new mass terms appear in the Hamiltonian. The relevant one is ee (others are $e\mu$, $e\tau$, $\mu\mu$, etc.)

$$\frac{M_{ee}^M}{2} (\bar{\nu}_{eL} \nu_{eR}^C + \text{H.C.}). \quad (11)$$

Obviously, this term violates the lepton number by two units ($\Delta L = 2$).

If the neutrinos are massive Majorana particles, a very rare process, the neutrinoless double beta decay ($0\nu 2\beta$), can occur in some nuclides. These are isotopes that are stable against normal beta decay, i.e. $Z \rightarrow (Z+1) + e^- + \bar{\nu}_e$ is forbidden, but with the two-neutrino double beta decay ($2\nu 2\beta$) channel open: $Z \rightarrow (Z+2) + 2e^- + 2\bar{\nu}_e$. This last is a very rare, but standard, second order weak process and occurs if the ground level of the Z isotope is lower than that of $Z+1$ but higher than that of $Z+2$.

Figure 6 shows the relevant graph of the process, where the cross in the neutrino propagator represents the Majorana mass term (11).

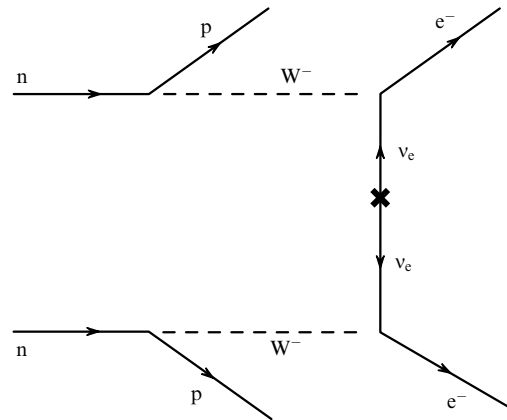


Figure 6. Neutrinoless double beta decay. Arrows indicate the flux of flavour.

The most common experimental approach is to measure the total energy released by the decay of the two electrons. Ideally, a spectrum as shown in Fig. 7 is expected: continuous for ($2\nu 2\beta$) decay, where some energy is taken by neutrinos, and a single line at the transition energy ($0\nu 2\beta$), where all the energy goes to the electrons. To exploit fully the advantage

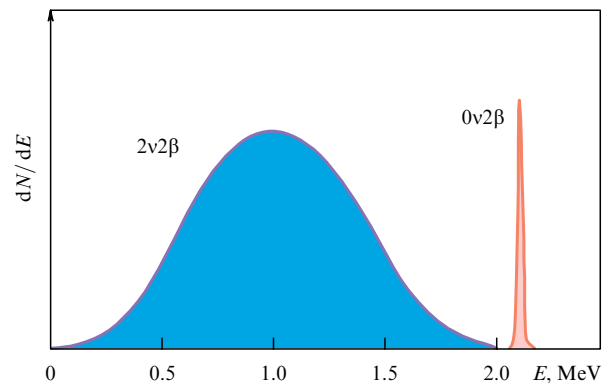


Figure 7. Double beta decay energy spectrum. E is the sum of the energies of the two electrons.

given by the monochromaticity of the signal, detectors must attain very good energy resolution that must be coupled with extremely low background conditions.

Up to now, no $(0\nu 2\beta)$ signal has been observed and limits on the corresponding lifetimes have been set. From each of them a limit on the electron-neutrino ‘effective mass’ M_{ee}^M can be extracted, taking into account the relevant nuclear matrix elements. The corresponding uncertainty for $\langle m_{\nu_e} \rangle$ is typically a factor of two. As a consequence, it is mandatory for a complete research program to include different double-beta active isotopes in the search.

In the present case, the ‘mass’ that is measured, or limited, is the quantity

$$|M_{ee}^M| = ||U_{e1}|^2 m_1 + |U_{e2}|^2 \exp(2i\alpha) m_2 + |U_{e3}|^2 \exp(2i\beta) m_3|. \quad (12)$$

Presently, the best limit, $M_{ee}^M < 0.34 \text{ eV}$ (90% CL), based on a half-life limit of 2.1×10^{25} years, was obtained by the Heidelberg–Moscow [8] experiment at Gran Sasso, with a 37.2 kg yr exposure of an enriched ^{76}Ge detector.

The same group proposed in 1997 the GENIUS [9] experiment, aiming for a forward jump in sensitivity with a large increase in enriched Ge mass (1000 kg) and a drastic reduction of the background. Naked enriched Ge crystals would be used in a liquid N_2 bath, 10 m across used both for cooling the crystals and screening external radioactivity. Monte Carlo calculations show that the technique should allow for a reduction in the background, in relevant energy, to $b = 3 \times 10^{-4}$ events $(\text{kg keV yr})^{-1}$. This would allow the experiment to reach the 10 meV neutrino mass range. To prove that such a large reduction in the background is possible in practice, Monte Carlo calculations are not enough: a series of tests is necessary. To this aim, the Collaboration has recently submitted the GENIUS-TF [10] proposal, based on 40 kg of natural Germanium, which promises some interesting measurements in itself. In particular, the present Heidelberg–Moscow crystals in this set-up can push the limit of the electron-neutrino mass to 100 meV over 6 years of data taking, if the background level $b = 6 \times 10^{-3}$ events $(\text{kg keV yr})^{-1}$ is reached.

The most sensitive experiment on a different isotope is MIBETA, again at Gran Sasso, with 20 TeO_2 crystals operating as bolometers at cryogenic temperatures. The total detector mass is almost 7 kg of natural Te or of 2.3 kg of the double-beta active ^{130}Te isotope (34% natural abundance). MIBETA has reached an exposure of 3.26 kg yr with a background level $b = 0.6$ events $(\text{kg keV yr})^{-1}$, giving the limit $M_{ee}^M < 2 \text{ eV}$ [11].

The next experiment with the same technique is CUORICINO [12] approved for 56 TeO_2 crystals, 0.76 kg each, corresponding to a total ^{130}Te mass of 14.3 kg. The first crystals are in the test phase. If the background level is reduced at $b = 0.1$ events $(\text{kg keV yr})^{-1}$, as appears to be feasible from the results of the tests, a sensitivity between 200 and 400 meV will be reached in M_{ee}^M .

A further increase in the mass, by an order of magnitude, and drastic reduction in the background are being studied in view of the CUORE project aiming to a 50 meV sensitivity. It will consist of 1000 natural Te crystals equal to those of CUORICINO with a sensitive ^{130}Te mass of 250 kg. To exploit the larger mass, a further reduction of the background is needed. With $b = 10^{-3}$ events $(\text{kg keV yr})^{-1}$ the limit will be $M_{ee}^M < 30 \text{ meV}$, while if the more conservative value of

$b = 10^{-2}$ events $(\text{kg keV yr})^{-1}$ is reached, $M_{ee}^M < 50 \text{ meV}$. As mentioned, CUORE is based on natural Tellurium, profiting from the high natural abundance of the double beta active ^{130}Te isotope. But enrichment is of course possible; if this is achieved without degrading the radio-purity, improvements by a factor 1.5 may be possible.

In conclusion, double beta decay experiments could reach sensitivities in the range, $M_{ee}^M = 30 - 50 \text{ meV}$. These are extremely interesting values. As the first example, let us consider the case of the solar SMA solution; then the mixing matrix is approximately given by Eqn (9) and from Eqn (12) $M_{ee}^M \approx m_1$. In this case already the present Heidelberg–Moscow result excludes neutrinos as cosmologically relevant in the universe.

As another example, take bi-maximal mixing and assume that m_3 is not too large; then, given the smallness of $|U_{e3}|$, the last term in Eqn (12) is small and we have

$$M_{ee}^M = \frac{1}{2} |m_1 + \exp(2i\alpha) m_2|. \quad (13)$$

Now, depending upon the value of α , cancellations can occur and the previous conclusion can be reached only if these are not important.

The hierarchic case is more difficult but notice that if the spectrum is ‘inverted’, then m_1 and m_2 will both be close to the square root of the atmospheric square mass difference, i.e. 40–70 meV. The sensitivity of GENIUS and CUORE might be enough to detect the signal.

Further contributions to the knowledge of neutrino masses and mixing can be made by Gran Sasso through the detection of supernova neutrinos. Neutrinos can practically be detected only for SN events in our galaxy or in Magellanian Clouds. The explosion produces neutrinos and antineutrinos of all three flavours in a burst lasting 20–50 s. Non-zero masses can lead to longer burst duration. The delay is given by

$$\Delta t = 5.15 \left(\frac{d}{10 \text{ kpc}} \right) \left(\frac{m_\nu}{1 \text{ eV}} \right)^2 \left(\frac{10 \text{ MeV}}{E_\nu} \right)^2 \text{ ms},$$

which is proportional to the square of the mass. The limit ‘ $m_\nu < 10 - 20 \text{ eV}$ ’ obtained from SN 1987A is limited mainly by the uncertainty of the neutrino ‘light’ curve and energy spectra and is difficult to improve.

The meaning of the effective neutrino ‘mass’ ‘ m_ν ’ is now again different. The neutrinos produced in the SN change their flavour while crossing the core or the ejecta via MSW effect. This changes both the fractions and the energy spectra of each eigenstate in the burst. The three eigenstates then move, with slightly different velocities, toward our detector. By measuring their arrival times we can only put a limit on a weighted average of m_1 , m_2 and m_3 with substantially unknown weights. These depend on the original composition, on the mixing matrix elements and on the detected flavour. They cannot give, as is frequently but wrongly claimed, a limit on, for example, the tau-neutrino mass. Flavour-sensitive and energy-sensitive detection of the neutrinos can on the other hand, give useful information on the mixing parameters, notably U_{e3} .

At Gran Sasso the LVD dedicated experiment, with its 1080 t sensitive mass of organic liquid scintillator, is mainly sensitive to electron antineutrinos through the process $\bar{\nu}_e + p \rightarrow n + e^+$. Between 300 and 600 events are expected for each SN explosion in the centre of the galaxy (8.5 kpc), followed by the neutron capture $n + p \rightarrow d + \gamma + 2.2 \text{ MeV}$,

used as a tag with 60% efficiency. The detector has a modular structure consisting of 912 tanks each seen by three photo-multipliers. The tanks are read out independently, so allowing a very high up-time, at least of a part of the apparatus. The up-time has been 99.3% during the year 2000.

Other processes will yield fewer events, as for example, only 6 events of the $\nu_e + {}^{12}\text{C} \rightarrow e^- + {}^{12}\text{N}$ process will be detected in the absence of oscillations. The yield is small, mainly because electron-neutrino energies are too low. But oscillations will convert the muon and tau neutrinos, which are produced with higher energies (roughly twice as high), into electron neutrinos, whose spectrum, as a consequence will become harder. The yield will increase to a few dozen events. We can thus obtain information on the mixing parameters.

In conclusion, detection of SN neutrinos can give very useful information about neutrino physics, mainly on mixing and (we have not discussed this point) the astrophysics of collapse. Very important will be the comparison of data obtained with different detectors, which have different sensitivity to energy and flavours. A global-warning network of different detectors is being set-up.

5. Neutrino oscillations. Contributions of Gran Sasso on atmospheric neutrinos

As already mentioned, Super-Kamiokande [14] observed an anomaly in muon neutrinos from the atmosphere that can be interpreted as evidence of neutrino oscillations. Super-Kamiokande is a large water Cherenkov detector with a fiducial mass of 22.5 kt. An electron neutrino or a muon neutrino interacting in the liquid produces an electron or a muon that has a direction similar to its own. The Cherenkov light cone produced by the charged lepton is detected as a ring by the photomultipliers that cover the walls of the detector. In this way, Super-Kamiokande detects in real time electrons due to electron-neutrino interaction and detects muons due to muon-neutrino interaction. Electron and muon neutrinos are produced by cosmic rays interactions in the atmosphere, then reach the detector crossing the earth with different path

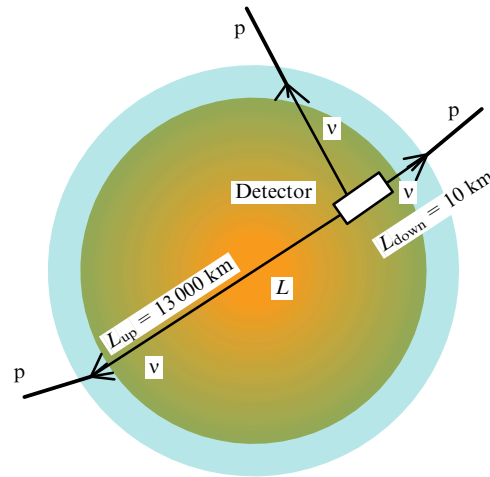


Figure 8. Correlation between incident angle and flight path for atmospheric neutrinos.

lengths. The measured direction gives the path lengths, as shown in Fig. 8.

Figure 9, left panel, shows that the flux of electron neutrinos is in accordance with expectations at all directions. Muon-neutrino flux, right panel, is as expected at short path lengths, becoming half of the expected at larger lengths. This disappearance phenomenon is interpreted as an oscillation with

$$1.5 \times 10^{-3} \text{ eV}^2 < \Delta m^2 < 5 \times 10^{-3} \text{ eV}^2,$$

given by the position of the step in the distribution. The corresponding oscillation period is short compared to 'solar' oscillations. As a consequence, at the L/E values involved in atmospheric oscillations, the second oscillation has not yet started and does not affect the data. The oscillation probability can be written as a good approximation (if also matter effects can be ignored) as

$$1 - P_{\nu_\mu \rightarrow \nu_\mu} = \sin^2(2\theta_{23}) \sin^2\left(1.27\Delta m^2 [\text{eV}^2] \frac{L [\text{km}]}{E [\text{GeV}]}\right).$$

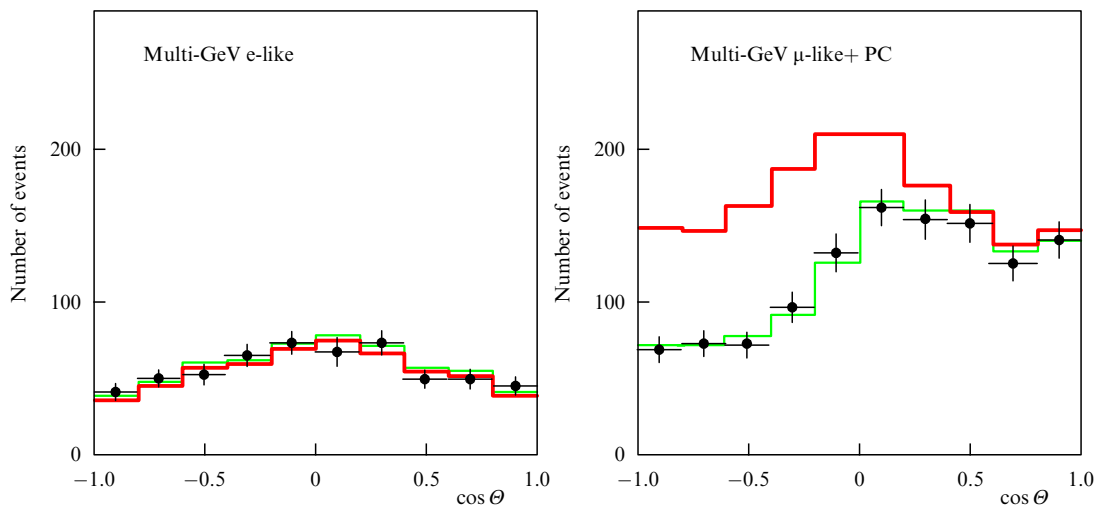


Figure 9. $\cos \theta$ distribution for the Super-Kamiokande 'Multi-GeV' events (dots). θ is the angle from the zenith of the charged lepton (electron or muon) detected in the apparatus. Heavy lines are predictions in the absence of oscillations, light lines are predictions for oscillations of muon neutrinos to tau neutrinos with $\Delta m^2 = 3.2 \times 10^{-3} \text{ eV}^2$ and $\theta_{23} = \pi/4$ (maximum mixing). Left panel is for electrons, right panel for muons.

This is identical to the expression (3) valid in a two-neutrino scenario, justifying the approximation in this case.

The height of the step in the angular distribution is close to 50%, meaning that the mixing is compatible with the maximum, (θ_{23} close to $\pi/4$).

The neutrino flavour (or flavours) into which muon neutrinos oscillate is not detected. It is not an electron neutrino, because this flavour behaves as expected, but is presumably a tau neutrino, given that these data are not sensitive to tau. A more exotic hypothesis is that the oscillation be into a neutrino species that does not interact with normal matter (and for this reason has never been observed), which is called a ‘sterile’ neutrino. Other Super-Kamiokande data, however, strongly disfavour this last hypothesis.

At Gran Sasso, this evidence has been confirmed with a complementary technique by the MACRO experiment. MACRO was a large area multipurpose detector used to search for rare events in cosmic radiation. It was built and commissioned gradually, in a modular structure, between 1988 and 1995 and took data until December 2000. The experiment yielded many important results but only those relevant to neutrino oscillations will be mentioned here.

The detector, shown in Fig. 10, had dimensions of $76.5 \times 12 \times 9.3 \text{ m}^3$, providing a capacity for isotropic flux of about $10\,000 \text{ m}^2 \text{ sr}$. Its mass was 5 300 t. The lower part of the detector contained ten horizontal planes of tracking chambers interleaved with rock absorbers; four more horizontal planes were located in the upper part. Vertical tracking planes were located on the side walls. Three horizontal planes of scintillator counters were located at the bottom and at the top of the lower part and, as a roof, over the upper part. The vertical sides were closed by scintillator planes.

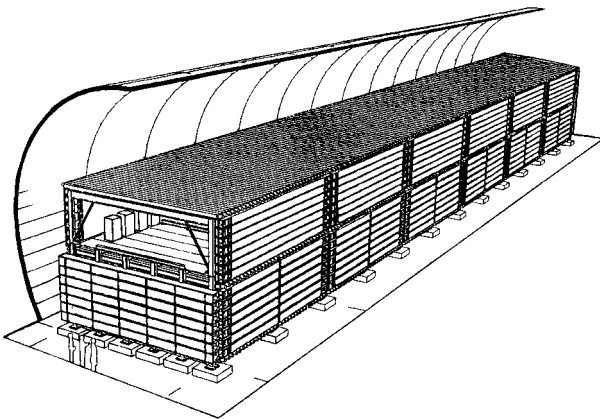


Figure 10. Sketch of the MACRO detector in Hall B.

Muons entering the detector from below were produced by interactions in the rocks of muon neutrinos that had been produced by cosmic rays in the atmosphere and had crossed the earth. The flight length of the neutrino could be inferred by its direction, as shown in Fig. 8, and is approximately given from the measured direction of the muon. Upward moving muons crossing the detector were identified by the tracking planes and by time of flight measured by the scintillator planes. They are very rare, less than 100 per year. The measurement of the time of flight gives the rejection factor of 10^7 necessary for a clean separation of the upward from the much more abundant downward moving muons. The latter

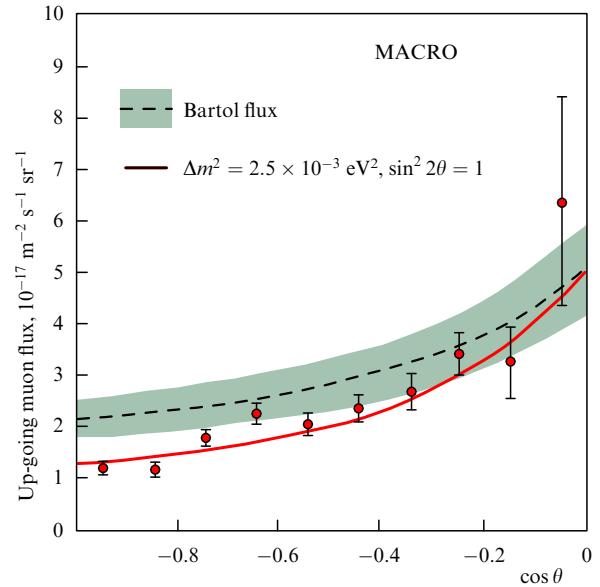


Figure 11. Angular distribution of the upward moving muons crossing the MACRO set-up. The angle is measured from the zenith. Continuous line is the expectation (band gives the uncertainty) in absence of oscillations. Dotted line is for the best fit with oscillations ($\Delta m^2 = 2.5 \times 10^{-3} \text{ eV}^2$ and $\theta_{23} = \pi/4$).

originate from the decay of mesons produced in the atmosphere by cosmic rays and constitute a huge background, even underground, where their flux is attenuated by a factor 10^6 .

Figure 11 shows the flux of muons that cross the detector coming from below [15] ($\cos \theta = -1$ is the nadir) compared with expectations. A clear deficit is observed at directions close to the vertical, i.e. for muon-neutrinos that have flown several thousands kilometres; their median energy is about 50 GeV. This phenomenon is interpreted as evidence of oscillations, with maximum mixing and $\Delta m^2 \approx 2.5 \times 10^{-3} \text{ eV}^2$ at the best fit point.

The ratio of vertical and horizontal fluxes is different if the oscillation is into tau or sterile neutrinos, at least for a range of values of Δm^2 . Figure 12 shows [16] this ratio defining as vertical flux for $-1 < \cos \theta < -0.6$ and as horizontal flux for $-0.6 < \cos \theta < 0$ as a function of Δm^2 . The tau-neutrino hypothesis is strongly favoured.

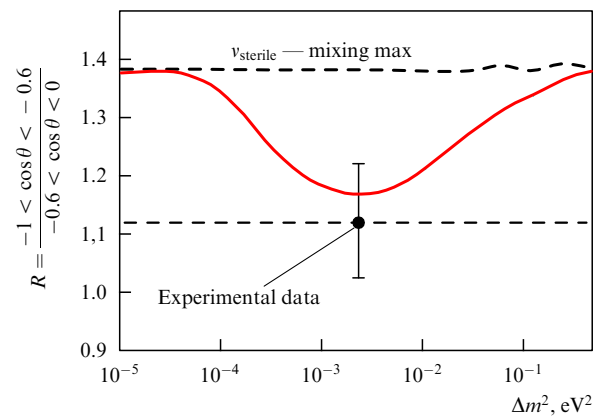


Figure 12. Ratio (R) between ‘vertical’ and ‘horizontal’ fluxes of upward moving muons. Curves show the expectations for muon neutrino oscillation 100% into tau-neutrinos and 100% into sterile neutrinos as functions of Δm^2 .

6. Neutrino oscillations. Contributions of Gran Sasso on solar neutrinos

The main process responsible for energy production in the sun is an overall reaction leading from four protons to a He nucleus, two positrons and two electron neutrinos. The process is called the pp chain. It produces an energy of 26.7 MeV. Because we know the energy flux from the sun and both the energy and the number of neutrinos produced by the above-mentioned elementary process, we can reliably calculate the expected electron-neutrino flux with an uncertainty of 2%.

But the situation is more complicated. There are other thermonuclear reactions that contribute very weakly to energy production but that give rise to neutrinos, as shown in Fig. 13. The most relevant are due to the ${}^7\text{Be}$ and to the ${}^8\text{B}$ branches.

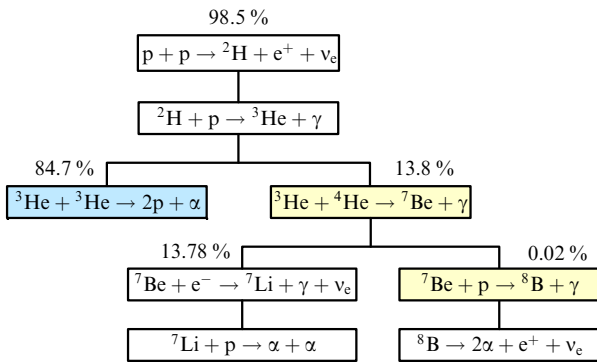


Figure 13. Branches of the pp cycle.

Figure 14 shows the calculated solar neutrino spectrum as predicted by the standard solar model [17]. In the upper part, the energy thresholds (the energy above which an experiment is sensitive) of the different experiments are reported. Notice that pp neutrinos have very low energies.

Homestake [18] was located in a mine in the US and took data between the 60's and 2001, when it was terminated. In the experiment solar electron-neutrinos were absorbed by the ${}^{37}\text{Cl}$ nuclei contained in 600 t of perchlorethylene. Homestake was the first experiment to detect solar electron-neutrinos and gradually discover a deficit in the neutrino flux. The energy

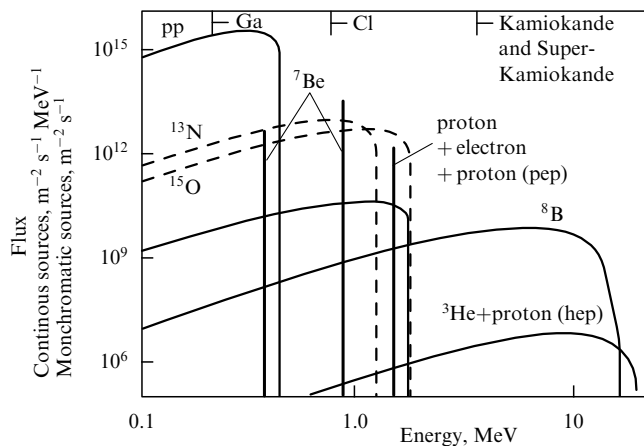


Figure 14. Solar neutrino spectrum.

threshold was 0.813 MeV and therefore the experiment was most sensitive to ${}^8\text{B}$ electron-neutrinos and modestly sensitive to ${}^7\text{Be}$ electron-neutrinos. Unfortunately, this experiment was never calibrated in its absolute efficiency. Its result is also the only solar neutrino experiment not yet independently confirmed.

Kamiokande [19] (data taking between 1985 and 1996) and its successor Super-Kamiokande [20] (started in 1996 and still running) are water Cherenkov detectors and detect in real time electrons recoiling from an elastic scattering of a neutrino. As a consequence, these experiments are sensitive to all neutrino flavours, even if with reduced sensitivity to ν_μ and ν_τ due their smaller cross sections. The threshold has been between 7 and 5 MeV so only the ${}^8\text{B}$ part of the solar spectrum is detected. Kamiokande was the first to show that neutrinos are really coming from the sun. Super-Kamiokande has confirmed the Kamiokande results with increased statistical (almost 20000 solar neutrino events have been collected so far) and systematic precision, measuring an electron-neutrino flux roughly half of that expected. This is known as the 'solar neutrino problem'. There are, in principle, two possible solutions: either the solar models we use are wrong (the astrophysical solution) or the neutrinos do not behave as predicted by the SM of the elementary particles (the particle solution).

Super-Kamiokande has also measured and continues to measure the neutrino energy spectrum both during the day and during the night, when neutrinos reach the detector crossing the earth and MSW effects are possible. An artificial electron source, an electron LINAC, is used by the experiment to calibrate accurately its energy scale.

The values predicted by the solar model in the higher energy part of the electron-neutrino spectrum strongly depend on the input parameters (even if severe constraints are imposed by our knowledge of the sun). On the contrary, as already stated the flux at low energy depends only on the solar luminosity. A process sensitive to these low energy electron-neutrinos is the absorption by ${}^{71}\text{Ga}$ nuclei, $\nu_e + {}^{71}\text{Ga} \rightarrow e^- + {}^{71}\text{Ge}$, whose threshold is 233 keV. The process is extremely rare, it occurring roughly once a day in 10 t of ${}^{71}\text{Ga}$ (30 t of natural Ga).

The resulting ${}^{71}\text{Ge}$, which are in an unstable state, are periodically extracted (every few weeks), detected via their decays and counted. GALLEX [21] at Gran Sasso and SAGE [22] in the Baksan Laboratory under the Caucasus² are based on this process and started data taking in 1991. GALLEX, that took data till 1997, uses 30 t of natural gallium in the form of a gallium-chloride solution (100 t), SAGE uses gallium in a metallic form.

The series of operations needed to extract and to count the very few nuclei is extremely delicate. A series of tests and checks of the efficiency was performed by GALLEX, including exposure to an artificial neutrino source that allowed to determine the overall performance of the procedure. The calibration source was a 62 PBq ${}^{51}\text{Cr}$ source giving electron neutrinos of energy similar to those from the sun (200 decays into ${}^{71}\text{Ge}$ in three months). For the ratio between measured and expected yield a run in 1994 gave $R = 1.0 \pm 0.1$, while a second run in 1995 gave $R = 0.83 \pm 0.1$. These measurements gave reason for strong confidence in the radiochemical technique.

² Baksan Neutrino Observatory of Institute for Nuclear Research, RAS.



Figure 15. A picture of the tank of GALLEX and GNO from the top.

Figure 15 shows from above one of the two tanks used by GALLEX and GNO. GALLEX was completed in 1997. GNO uses the GALLEX structures with 30 t of natural Ge and with several improvements in the counters and the electronics (a substantial increase in Ga mass has been proposed). It will continuously take data for a long period (around 10 years), gradually reducing the overall uncertainty

in the flux measurement below 5%. For some solutions, seasonal variations might be observable. The result of the first run have been published [23] with a measured yield of $65.8^{+10.2}_{-9.6}$ (stat) $^{+3.4}_{-3.6}$ (syst), the systematic uncertainty being already reduced to 5.3%. These results, together with those of GALLEX (divided into four periods), are shown in Fig. 16. For comparison, the solar model predictions range between 115 and 135 SNU. A strong deficit is observed.

Similar results have been obtained by the SAGE experiment that, while based on the same physical process, use completely different techniques with different uncertainties and systematic errors. The agreement between the two experiments strongly enhances the reliability of the result.

These observations not only confirmed the solar neutrino problem, but lead to the exclusion of the astrophysical solution. In fact, the flux measured by GALLEX is mainly the sum of the pp, ${}^7\text{Be}$ and ${}^8\text{B}$ contributions. If one subtracts the pp flux as calculated from solar luminosity and the ${}^8\text{B}$ contribution as measured by Super-Kamiokande from the total flux as measured by GALLEX (and SAGE too) one finds that no room at all is left for Be neutrinos. But Be neutrinos must exist because Be is a daughter of B (see Fig. 13). This is a second anomaly, known as the ‘Be neutrino problem’. There is no astrophysical process to explain the absence of Be neutrinos and the only explanation left is that electron neutrinos disappear as such in their journey from the centre of the sun to the earth. The most probable interpretation is that neutrinos change their flavour by oscillations in the vacuum or by the MSW effect in the sun or both.

To summarise, all the experiments (Homestake, Kamio-kande, Super-Kamiokande, GALLEX, SAGE, and GNO) show important deficits of electron-neutrino flux in different parts of the solar neutrino spectrum, as shown in Table 1.

Super-Kamiokande has also provided accurate measurements of the higher energy part of the spectrum and of the ratio of the diurnal and nocturnal fluxes.

As we have already noted, there are two physical effects that contribute to neutrino flavour conversion. One is oscillation in a vacuum, the other is the MSW effect in matter. Electron neutrinos are produced in the core of the sun, then fly 700 000 km along its radius in a variable density

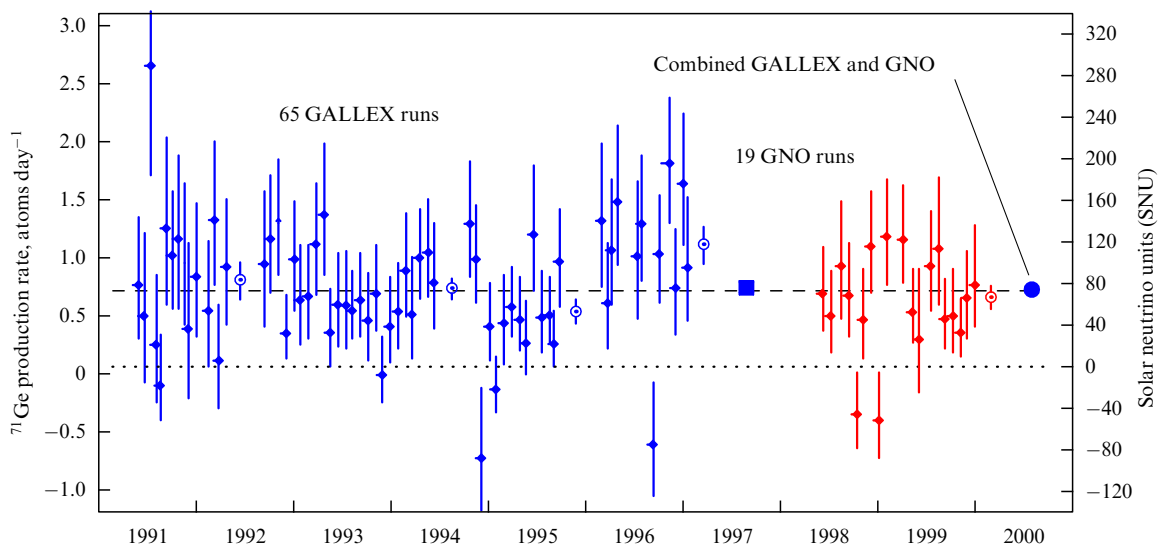


Figure 16. The yield measured by GALLEX and GNO. It is given by the product of the electron-neutrino flux and of the capture cross-section integrated over the relevant energy range. One ‘solar neutrino unit’, SNU = 10^{-36} captures per target nucleus per second.

Table 1. Energy thresholds and observed signal as a fraction of the expectations for the solar neutrino experiments.

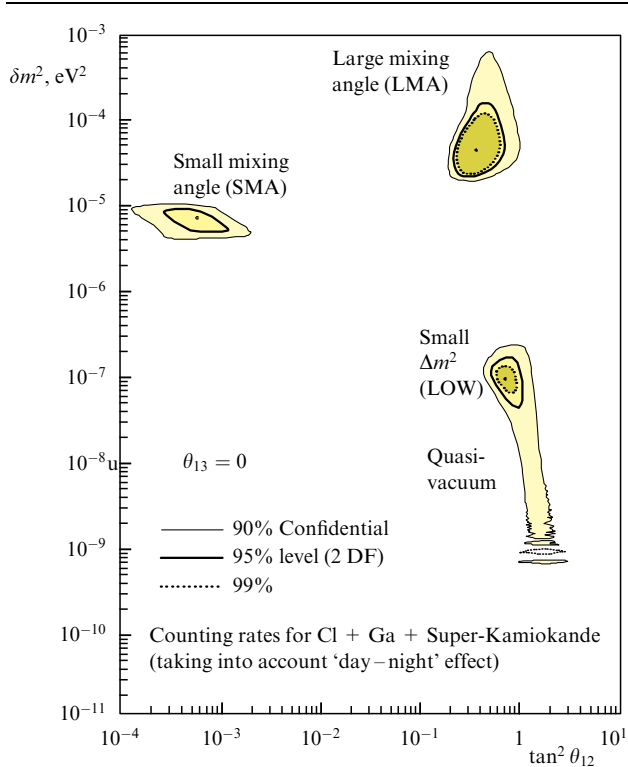
	Homestake	Kamiokande	Super-Kamiokande	GALLEX	SAGE
Threshold, MeV	0.814	7.5	6.5	0.233	0.233
Fraction observed, %	33 ± 6	55 ± 12	47 ± 8	60 ± 7	52 ± 7

medium. For some values of the oscillation parameters matter effects can sufficiently enhance the electron-neutrino disappearance probability even for small mixing.

Then neutrinos, the eigenstates, propagate in a vacuum for 150 000 000 km and reach our detector directly, during the day, after having crossed the earth (again with possible MSW) during the night. Again, for some values of the parameters, matter effects in the earth can enhance flavour conversion, resulting in a difference between diurnal and nocturnal fluxes. This day-night effect would be direct evidence of oscillations but has not yet been observed. This excludes those parameters that imply large day-night differences.

G Fogli and collaborators [24] have made a global fit of all the data. The propagation times to cross the sun and to fly from the sun to the earth are both much longer than the ‘atmospheric’ oscillation period, so that the effect of this oscillation averages out and does not affect the data. We also know that θ_{13} is very small; we will therefore report here only the fit for $\theta_{13} = 0$, which in any case gives practically all the relevant information.

The results are shown in Fig. 17: three different solutions, dominated by the MSW effect (in the sun) are present: SMA, LMA and LOW. In the lower part of the LOW solution, the contributions of the oscillations in a vacuum become important and the authors call this phenomenon ‘quasi vacuum’. Notice, in particular, the (anticipated) asymmetry between $\theta_{12} \geq \pi/4$ and $\theta_{12} \leq \pi/4$.

**Figure 17.** Solutions of the solar anomaly.

There is a further possibility, that of pure oscillation in the vacuum. For this to happen, the distance between the sun and the earth must be just right and, for this reason, it is sometimes called the ‘JUST SO’ solution. Clearly, in this case seasonal effects are expected due to the small (7%) eccentricity of earth’s orbit. This solution is not favoured by present data and is not included in Fig. 17, but it is not yet completely excluded. Its δm^2 is very low, between 10^{-10} and 10^{-12} eV² and mixing close to maximum.

A final observation is the following. Electron neutrinos produced in the sun disappear in part before reaching our detectors. If they oscillate, in which final state they do? We don’t know the answer, but if the mixing matrix is bi-maximal the other state is a fifty-fifty quantum superposition of muon neutrinos and tau neutrinos

$$\nu_{\mu\tau} = \frac{1}{\sqrt{2}}(\nu_{\mu} + \nu_{\tau}).$$

The solar model calculations need the values of the cross sections of the nuclear reactions involved in the different branches of the pp cycle. These cross sections are so small, due to the extremely low Coulomb barrier penetration probability at the relevant energies (called the Gamow peak), that their measurement only recently became possible in the low background Gran Sasso environment. The LUNA experiment is based on a 50 kV ion accelerator located underground at Gran Sasso Laboratory, providing a high intensity beam (${}^3\text{He}^+$, 500 mA) on a windowless target. It has already measured the cross section of the important ${}^3\text{He} + {}^3\text{He} \rightarrow 2\text{p} + {}^4\text{He}$ reaction (see Fig. 13). The cross section drops almost exponentially with decreasing energy and can be written in the form

$$\sigma(E) = \frac{S(E)}{E} \exp\left(-31.3Z_1Z_2\sqrt{\frac{\mu}{E}}\right),$$

where μ is the reduced mass in units of amu, Z_1 and Z_2 are the charges of the nuclei and E is the centre of mass energy in keV. The $S(E)$ is called the astrophysical factor and is used to extrapolate at low energies, assuming a smooth behaviour. This would not be the case in the presence of a resonance.

Figure 18 shows the LUNA results down to 17 keV [25] (where the rate was 2 events/month!) below the Gamow peak. No resonance is present. One can also notice the effect of shielding by the atomic electrons. At these low energies the wavelengths of the nuclei of the beam have atomic scale values and ‘see’ a target nucleus surrounded by electrons as a single unresolved object. As a consequence, its effective charge is reduced and with it the Coulomb repulsion.

The LUNA2 experiment has been approved and its 400 kV accelerator is now in operation. A new BGO-4 π -summing detector, consisting of six optically separated segments, each observed by two photomultipliers at either side, completes the new facility. The gas target is located inside a bore-hole of the BGO detector. A good energy resolution is indeed essential to reduce the background.

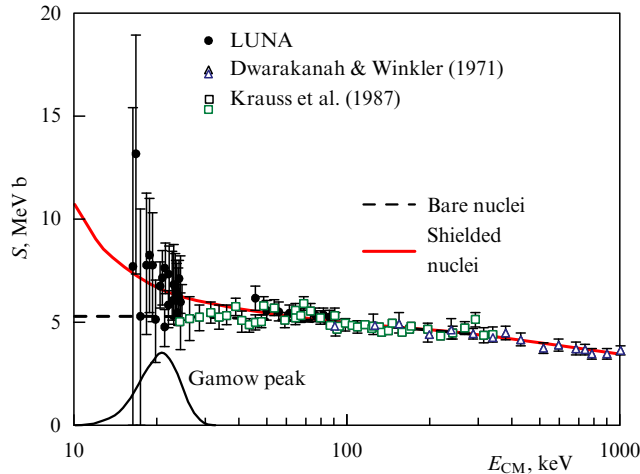


Figure 18. Astrophysical factor S for the reaction as measured by LUNA at Gran Sasso. Higher energy data from other experiments are also reported.

Starting in 2001, the reactions $^{14}\text{N}(p, \gamma)^{15}\text{O}$, $^3\text{He}(^3\text{He}, \gamma)^7\text{B}$ and $^7\text{Be}(p, \gamma)^8\text{B}$ will be studied.

7. The next steps

In the previous sections, I have briefly described recent experimental findings that have generated the new neutrino physics, with special emphasis on the contributions of the Gran Sasso Laboratory. We might just be entering a new field that promises new discoveries in the future. The program over the next years should include experiments to:

A. Observe oscillation signals for both the atmospheric and the solar anomalies. In neither case have we observed a non-ambiguous sign of oscillation. In both cases oscillations give the simplest explanation, but more exotic interpretations can not be excluded.

B. Confirm the atmospheric neutrino oscillation observation with experiments on a neutrino beam produced at a far away accelerator. This step is mandatory because the flux of atmospheric neutrinos is not under our control and is known only through Monte Carlo calculations, whereas the composition (mainly muon neutrinos) and the energy spectrum of an artificially-produced beam are under control. Both muon-neutrino disappearance and tau-neutrino appearance experiments are planned. The K2K experiment has been running since 1999: a muon-neutrino beam is produced at the KEK and is sent to the Super-Kamiokande detector 250 km away. The low neutrino energies (2–3 GeV) give good sensitivity even with low statistics. The first evidence of oscillations has already been reported but further data are eagerly awaited [26].

The NUMI program at Fermilab is building a muon-neutrino beam to shoot at the MINOS detector being built in the Soudan mine 730 km away in Minnesota. The experiment is planned to start data taking at the end of 2003 in a disappearance mode [27].

C. Discover if the flavour into which atmospheric ν_μ oscillate is indeed ν_τ or else with a ν_τ appearance experiment as planned by the CNGS project in Europe (see below). This issue is clearly connected with the existence of low mass sterile neutrinos coupled to known particles.

D. Improve the knowledge of mixing parameters.

E. Measure the sign of Δm^2 . Is the spectrum ‘normal’ or ‘inverted’? In this context we have already discussed the possibility of searching for $0\nu 2\beta$.

F. Improve the knowledge of δm^2 . Choose solar solution.

G. Detect, if it exists, the $\nu_\mu \leftrightarrow \nu_e$ oscillation at Δm^2 . Is $U_{e3} \neq 0$?

H. Search for CP violation in the lepton sector. This is extremely difficult, for a number of reasons, including the fact that the effects are suppressed by the factor $\delta m^2/\Delta m^2 \ll 1$ and by the smallness of $|U_{e3}|$.

I. Determine the nature of neutrinos: Majorana or Dirac?

J. Measure the absolute values of the masses.

Experiments at Gran Sasso Laboratory can make important contributions, provided that we are able to build a coherent program. This will be done on the basis of the many interesting ideas and proposals that have been submitted and that are in different stages of development and of the resources that will become available. In the following sections I will briefly describe these proposals.

8. Neutrinos from CERN

An important component of the program will be the CNGS project. An artificial, well-controlled neutrino source will be built at CERN for experiments at LNGS. Both the beam and the experiments will be optimised for ν_τ appearance. A CERN–INFN group has designed the neutrino beam [28]. The pions and kaons produced by the 400 GeV SPS proton beam will be focused by a two horn system, followed by a 1 km long decay tunnel, a hadron stop, and muon detectors for beam characteristics determination. The resulting beam is almost pure in muon neutrinos, with a small contamination of the other flavours, the most important being electron neutrinos, that is $\approx 0.8\%$.

The optimum L/E value for observing ν_μ oscillations is given by Eqn (2) and for $\Delta m^2 = 3.5 \times 10^{-3} \text{ eV}^2$ is $(L/E)_{\text{max}} \approx 300 \text{ km GeV}^{-1}$. At a distance of 730 km (that from CERN to Gran Sasso and from Fermilab to Soudan), the energy for maximum oscillation is $E_{\text{max}} \approx 2.5 \text{ GeV}$. This is indeed the optimum energy for disappearance experiments but not for ν_τ appearance experiments, as much as tau leptons must be produced through the reaction

$$\nu_\tau + N \rightarrow \tau^- + N'.$$

This requires neutrino energy to be above the threshold ($\approx 3.5 \text{ GeV}$) for tau production, in practice larger than $\approx 10 \text{ GeV}$. Figure 19 shows the neutrino fluence at Gran Sasso for the CERN beam compared with the product of the oscillation probability (decreasing with increasing energy) and the τ production cross section (increasing with energy). One can see that the beam spectrum is optimised for appearance at the Gran Sasso site.

The ν_τ appearance probability in an initially pure ν_μ beam of energy E is

$$P_{\nu_\mu \rightarrow \nu_\tau} = \sin^2(2\theta_{23}) \cos^4(\theta_{13}) \sin^2\left(1.27\Delta m^2 [\text{eV}^2] \frac{L [\text{km}]}{E [\text{GeV}]}\right).$$

As $\theta_{13} \approx 0$, we have approximately

$$P_{\nu_\mu \rightarrow \nu_\tau} = \sin^2(2\theta_{23}) \sin^2\left(1.27\Delta m^2 [\text{eV}^2] \frac{L [\text{km}]}{E [\text{GeV}]}\right).$$

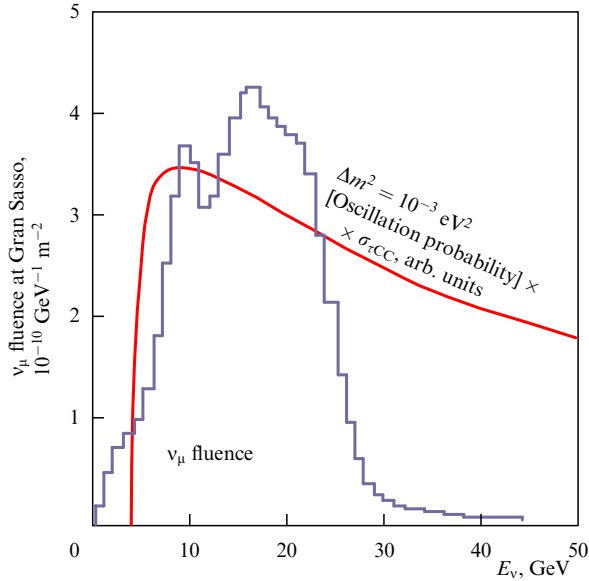


Figure 19. Neutrino fluence at Gran Sasso for the CERN beam compared with the product of the oscillation probability and the τ production cross section for $\Delta m^2 = 10^{-3} \text{ eV}^2$.

Even in this case, the commonly used two-neutrino approximation is justified as long as we ignore the minority muon-neutrino to electron-neutrino oscillation.

A nearby detector station is not needed for appearance experiments. Running in the ‘shared’ mode, the beam will give 3200 CC ν_μ interactions per year in a kiloton fiducial mass detector at LNGS corresponding to 25 ν_τ interactions for $\Delta m^2 = 3.5 \times 10^{-3} \text{ eV}^2$ and maximum mixing (1.7 times more in dedicated mode operation).

The charged daughters of τ 's will be detected in one or more decay channels: $\tau^- \rightarrow \mu^- \nu_\mu \nu_\tau$ (18%); $e^- \nu_e \nu_\tau$ (18%); $h^- \nu_\tau n \pi^0$ (50%); $2\pi^- \pi^+ \nu_\tau n \pi^0$ (14%). Two main background rejection tools are available: (1) The direct observation of τ decays requiring micrometer scale granularity and sub-micron resolution. These are possible only by means of the emulsion technique (as used by CHORUS and DONUT and proposed by OPERA); (2) The use of kinematic selection, which requires good particle identification and good resolution of momentum imbalance (as used by NOMAD and proposed by ICARUS).

ICARUS [29] is a liquid argon time projection chamber providing bubble chamber quality 3D images of the events, continuous sensitivity, self-triggering capability, high granularity calorimetry and dE/dx measurement. The R&D program performed between 1991 and 1995 on a 3 t detector solved all the major technical problems with the detector continuously running for several years, showing the reliability of the technique.

The present phase aims to demonstrate the feasibility of a medium-scale detector. A 600 t unit composed of two 300 t units is presently being constructed in Pavia. The two 300 t units will be completely assembled and tested before being separately transported to Gran Sasso. Presently, one 300 t unit has been completed (see Fig. 20) and is now expected to be operational by mid-2001. This will be the main milestone in the program. The safety issues connected with the underground installation of a large cryogenic volume are also being studied. The project comprises the construction of a large modular detector to



Figure 20. Inside the 300 t ICARUS sub-module, a view of one of the two mirror drift volumes. The presence of the wire chambers on the left can be inferred from the oblique pattern on the left due to the reflection of light.

cover a broad physics program, of which I'll discuss only the CNGS part.

The electron channel will be the main, although not the only, means used in the ICARUS search for τ appearance, carried out mainly by searching for an excess at low electron energies will make that. Due to the ν_e component of the beam ($< 1\%$) the background will be small. The superior e/π^0 separation capability will be exploited to cut out ν_μ neutral current events. Figure 21 shows the visible energy distribution as expected in a 20 kt yr exposure for $\Delta m^2 = 3.5 \times 10^{-3} \text{ eV}^2$ and maximum mixing. After kinematic cuts, 29 τ events will be detected, for $\Delta m^2 = 3.2 \times 10^{-3} \text{ eV}^2$ (best fit of Super-Kamiokande data) and maximum mixing ($\theta_{23} = \pi/4$) with a residual background of 5 events. Figure 22 shows the discovery potential of the experiment as statistical significance as a function of the exposure. If the systematic uncertainty in background calculation presently being studied will, as expected, not be large, a 20 kt yr exposure will have discovery potential more than 4σ for $\Delta m^2 > 2 \times 10^{-3} \text{ eV}^2$, as shown in Fig. 22.

The superior capability of detection and energy measurement of electrons at ICARUS can be used to search for the minority $\nu_\mu \leftrightarrow \nu_e$ oscillation component. Notice that the commonly used two-state formalism is misleading here due to the fact that the ‘mixing parameter’, $\sin^2 2\theta$, has different meanings in the disappearance (CHOOZ) and appearance (ICARUS, MINOS) cases. In a disappearance experiment, the maximum electron-neutrino disappearance probability is

$$P_{\max}(\nu_e \text{ disappearance}) = \sin^2(2\theta_{13}) \approx 4\theta_{13}^2 = 4|U_{e3}|^2$$

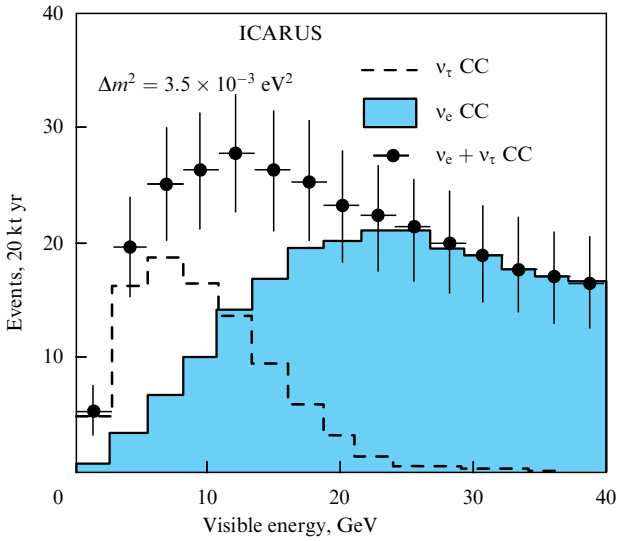


Figure 21. Visible electron energy distributions as calculated for a 20 kt yr exposure of ICARUS (the actual calculation is for a much larger exposure, but the indicated statistical uncertainties are for 20 kt yr). The contributions of electrons produced by ν_e 's originally present in the beam and by ν_τ 's generated by the oscillation are separately shown ($\Delta m^2 = 3.5 \times 10^{-3} \text{ eV}^2$ and maximum mixing).

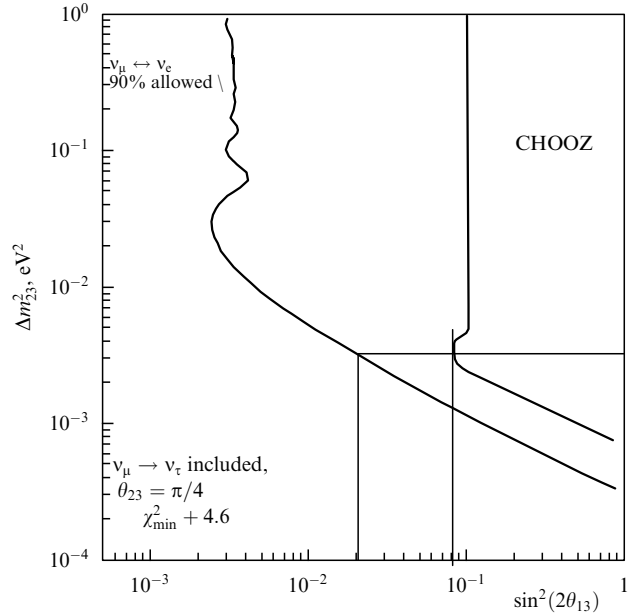


Figure 23. Exclusion plot for a 20 kt yr exposure of ICARUS at CNGS beam shown in the for Δm^2 vs. $\sin^2(2\theta_{13})$ plot compared with the CHOOZ limit. $\theta_{23} = \pi/4$ is assumed. The lines I added help to see the limits reached by CHOOZ and possible for ICARUS in the assumed conditions.

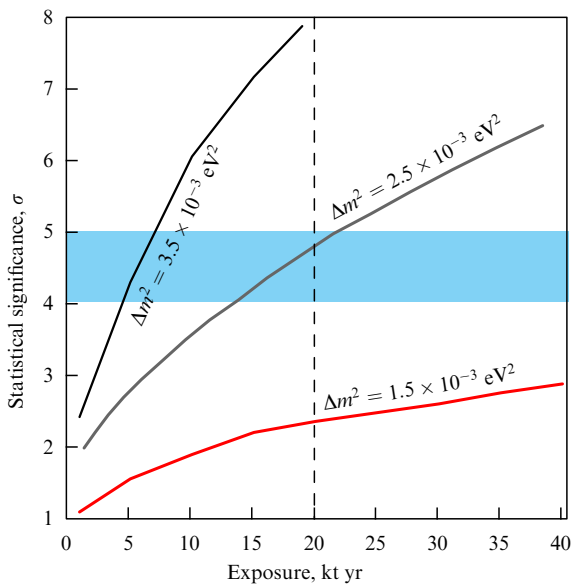


Figure 22. Discovery potential of ICARUS as a function of the exposure for different values of for Δm^2 (adapted from [29]).

where we take into account the smallness of θ_{13} . In an appearance experiment, the maximum electron-neutrino appearance probability is [see Eqn (7)]

$$P_{\max}(\nu_\mu \rightarrow \nu_e) = \sin^2(2\theta_{13}) \sin^2(\theta_{23}) \approx 4\theta_{13}^2 \frac{1}{2} = 2|U_{e3}|^2$$

where we used the approximately known value of $\sin^2(\theta_{23})$.

As a consequence, under the same conditions, the disappearance experiment is twice as sensitive to $|U_{e3}|^2$ as the appearance experiment. The physical reason is that in the former case, we do not look at the final state, which is about a fifty-fifty linear combination of muon neutrinos and tau neutrinos, while in the latter case we know that the initial state is purely muon neutrinos. Taking into account these

considerations, one can expect from the ICANOE experiment [29] an improvement on the present limit on $|U_{e3}|^2$ by about a factor of two, depending on the systematic errors, with a 20 kt yr exposure. This limit can be improved by another factor two if we take into account the electron energy spectrum [30] as shown in Fig. 23.

For a more substantial improvement, one would need a $\nu_\mu \leftrightarrow \nu_e$ appearance experiment at the first oscillation maximum. At the CERN to Gran Sasso distance, the optimum neutrino energy is low 2–3 GeV. In this case, the appearance of ν_e , has no threshold so that the low energy is adequate. What is needed is a high intensity, low energy ν_μ source and a detector of several kilotons. This possibility deserves further study [31].

Both INFN and CERN have recently approved OPERA [32]. Its design is based on the ECC concept, which combines in one cell the high precision tracking capability of nuclear emulsion and the large target mass afforded by lead plates. Figure 24 shows the cell structure (1 mm thick Pb plates followed by a film made up of two emulsion layers 50 μm thick on either side of a 200 μm plastic base). Two topologies of τ events are shown: ‘long’, where the τ production and decay are separated by at least one film (detected via the decay angle), and ‘short’, where they are not (detected via impact parameter).

The basic building block of the target structure is a ‘brick’, a sandwich of contiguous cells enclosed in a light-tight envelope. The envelope is evacuated thus obtaining the help of atmospheric pressure to keep the emulsion and Pb sheets firmly in place. The bricks are assembled into ‘walls’, vertical planar structures. Each wall is followed by electronic trackers with a moderate resolution with the scope to identify the brick where a neutrino interaction took place (a ‘fired’ brick) and to guide off-line scanning. The wall structure plus trackers is called a ‘module’. Fired bricks will be removed and processed (involving alignment, development and scanning of the emulsion sheets) on a daily basis.

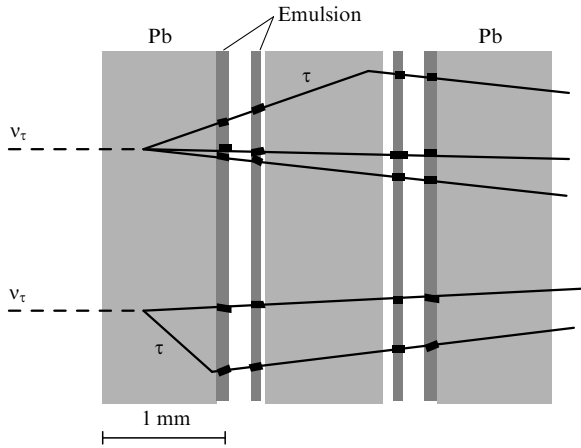


Figure 24. Basic cell of OPERA showing a ‘long’ and a ‘short’ event topology.

Accuracy in the measurement of the transverse momentum of the daughter particle (muon, electron, or hadron) is very important to reduce the background. The momenta of the muons will be measured by dedicated spectrometer, consisting of a dipole magnet (1.5 T field) and precision trackers (drift tubes). The energy (momentum) of electrons will be determined from the shower development, sampled by tracker planes (RPC). The momentum of the charged hadrons will be measured by studying multiple scattering in the emulsion sandwich.

A series of modules (brick wall and trackers) and its downstream spectrometer constitutes a super-module. Three super-modules constitute the full OPERA detector, with a total fiducial mass of 2 kt.

The ECC technique, which has recently led DONUT to discover the ν_τ , will be further developed. The necessary 176 000 m² of emulsion sheets will be produced industrially with an automatic chain and a new generation of automatic scanning/measuring devices will be produced through the collaboration. All the one-prong decay channels will, almost evenly, contribute to the final OPERA statistics. In a five year run, 18 identified τ decays with 0.6 background events are

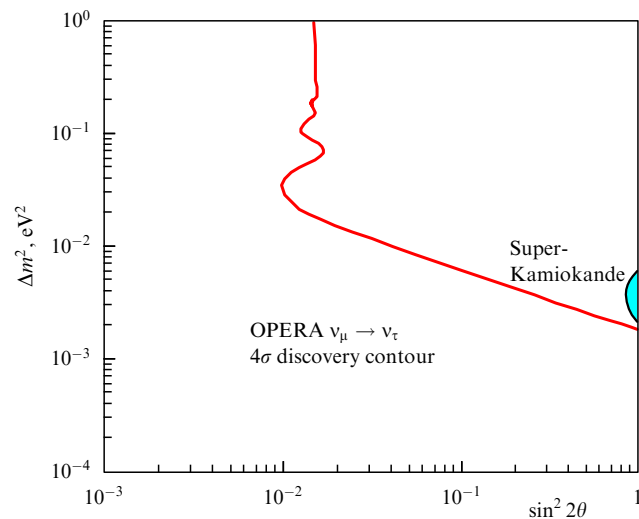


Figure 25. Discovery limit at 4σ of OPERA in a 5-year exposure in the shared mode. θ in the abscissa is θ_{23} .

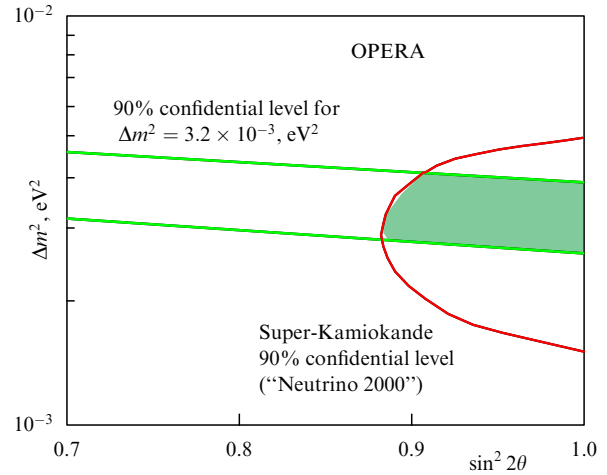


Figure 26. The horizontal band shows the OPERA result after 5-year data taking if $\Delta m^2 = 3.2 \times 10^{-3} \text{ eV}^2$. θ in the abscissa is θ_{23} .

expected for $\Delta m^2 = 3.2 \times 10^{-3} \text{ eV}^2$ (the best fit of Super-Kamiokande data), 44 for $5 \times 10^{-3} \text{ eV}^2$ and 4 for $1.5 \times 10^{-3} \text{ eV}^2$. Notice that there is still space to optimise the beam performance opening the possibility to increase these yields. Figure 25 shows the 4σ discovery limit.

Experiments on a beam cannot determine Δm^2 separately from the mixing angle, but give only the relationship between them. This is shown as a band in Fig. 26, together with the present Super-Kamiokande result.

9. Atmospheric neutrinos

Atmospheric neutrino experiments are complementary to CNGS. As we have already seen, the expected rate of tau neutrinos rapidly decreases with decreasing values of Δm^2 [more precisely, it is directly proportional to $(\Delta m^2)^2$] and is already very low at the smallest values in the range of Super-Kamiokande (around $1.5 \times 10^{-3} \text{ eV}^2$). The problem arises because the L/E values of the CNGS project are still small compared to the oscillation half-period. Atmospheric neutrinos, on the other hand, have flight lengths ranging from a few kilometres to 13 000 km and energies from fractions of GeV to many GeV, corresponding to a wide range of L/E (flight time) values. The conclusion is that if Δm^2 happens to be too small, say below $(1-2) \times 10^{-3} \text{ eV}^2$, an experiment on cosmic rays may be the only tool.

To improve on Super-Kamiokande, one must measure as accurately as possible the muon-neutrino energy E and its flight length L , to have L/E . L is obtained from the neutrino direction, inferred from the measured μ direction. To have a good correlation, one must use only μ 's above a GeV or so, were the cosmic ray flux is low. As a consequence, several kiloton mass detectors with coarse resolution are needed. The MONOLITH [33] proposal is a 35 kt spectrometer made of 8 cm thick horizontal Fe magnetised (1.3 T) plates. The interleaved tracking planes have 1 cm spatial resolution and good (1 ns) timing, for up/down discrimination.

For a given direction, downward moving ν_μ do not oscillate, while upward moving ν_μ do. The ratio between the two fluxes is known with small systematic uncertainty. Its measurement as a function of the angle at MONOLITH's highest L/E resolution will allow for the detection of the first

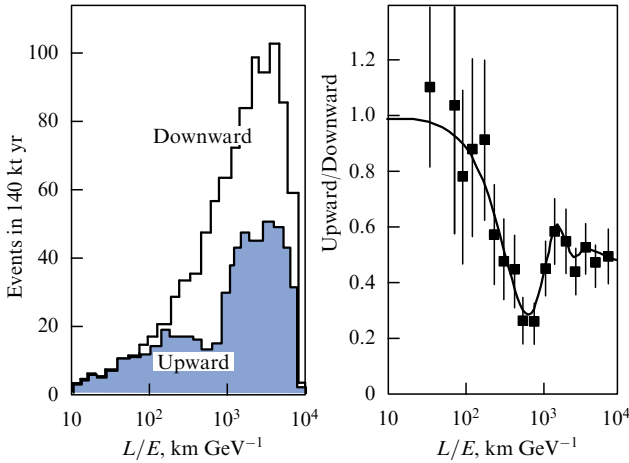


Figure 27. MONOLITH. Expected downward and upward muon fluxes (left panel) and the ratio of the two fluxes vs. L/E for 140 kt yr exposure.

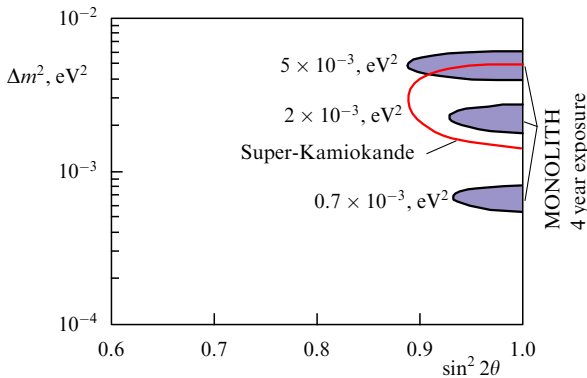


Figure 28. Expected MONOLITH results in a 4-year exposure (140 kt yr) in three different hypotheses on Δm^2 compared with the present Super-Kamiokande result. θ in the abscissa is θ_{23} .

oscillation period, as shown in Fig. 27, for $\Delta m^2 = 5 \times 10^{-3} \text{ eV}^2$.

MONOLITH will also result in a substantial improvement in the knowledge of Δm^2 , as shown in Fig. 28 for a 140 kt yr exposure.

Notice that the oscillation pattern becomes wider when Δm^2 decreases. As a consequence, experiments on atmospheric neutrinos become easier for lower Δm^2 values, contrary to those on a beam from an accelerator.

10. Solar neutrinos

Solar neutrino physics will be another important component of the program: GNO is taking data, BOREXINO [34] is completing its construction and will be ready to take data early in 2002, and LENS is in its R&D phase.

As already stated, GNO is planned to run for several years, gradually reducing statistical and systematic uncertainties. This will be very important by itself. Notice in particular that, given the final GALLEX result of $77.5 \pm 8 \text{ SNU}$ and an absolute minimum of 80 SNU as evaluated from sun luminosity, GNO, with reduced errors (and some luck), might become able to exclude by itself the astrophysical solution. Seasonal variations might be observed in the case of the vacuum or LOW solutions.

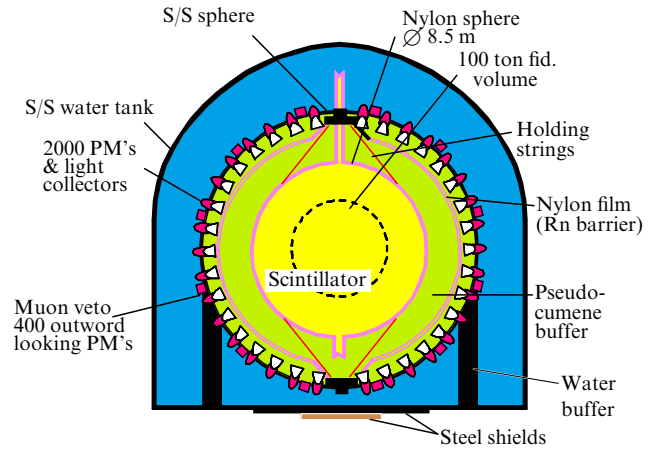


Figure 29. Sketch of the BOREXINO detector.

As we have already said, Be neutrino flux appears to be particularly sensitive to neutrino oscillations parameters. The measurement of this mono-energetic, 0.86 MeV, flux in real time is the principal aim of the BOREXINO experiment. Electrons resulting from neutrino (any flavour, but with ν_μ and ν_τ cross sections smaller than ν_e) scattering in the liquid scintillator detector medium will produce a light flash that will be detected by photomultipliers. 300 t of ultra-pure pseudocumene will be contained in a nylon sphere, the 100 t innermost mass being the sensitive volume. A larger volume of pseudocumene inside a 13.7 m diameter stainless steel sphere hosting the optical modules surrounds the nylon sphere. This sphere is immersed in a tank of 2500 t of purified water (Fig. 29).

Figure 30 shows a picture of the interior of the stainless steel sphere with scaffold which will be used for installation of the photomultipliers.

Taking into account that the energy spectrum of the recoiling electrons is on a continuum up to 0.66 MeV, the experiment is designed with a threshold of 0.25 MeV. The main problem at such low energies is the control of the background due to ever present radioactive isotopes. An intense R&D program has been carried out in the last ten years to select materials and to purify them at unprecedented limits of radio-purity. In parallel, techniques have been developed to measure ultra-low levels of radioactivity. Record levels of $10^{-16} - 10^{-17}$ (g of contaminant/g of material) for ^{232}Th and ^{238}U have been achieved.

The neutrino yield from Be is extremely sensitive to the oscillation parameters. The yield is 40 events/day for the standard solar model. Figure 31 shows electron-neutrino survival probabilities for the three MSW solutions. The large differences will allow for discriminating amongst them. In particular, for the SMA solution, the expected electron-neutrino flux is zero but BOREXINO will still count the interactions induced by the flavour in which the electron neutrinos have oscillated.

If Δm^2 is sufficiently low, say $< 10^{-8} \text{ eV}^2$ as in the ‘vacuum’ solution, strong seasonal variations are expected as shown in Fig. 32.

I believe that even more is needed for a complete program on solar neutrino physics, namely we need to measure in real-time the neutrino spectrum in order to separate the contributions of the different branches, pp, ^7Be , pep, ^8B , and CNO. Such an experiment should provide flavour sensitivity too, at least in combination with other experiments. The only

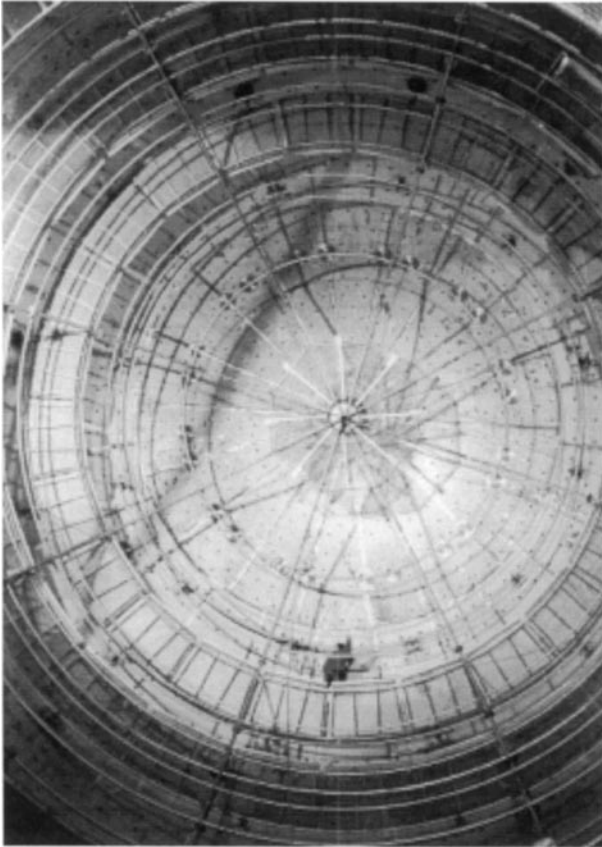


Figure 30. Inside the sphere, with scaffold for PM's installation.

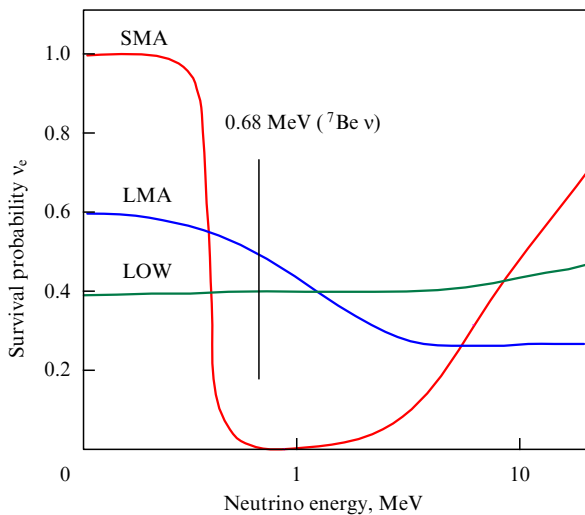


Figure 31. Survival probability for electron-neutrinos as functions of energy for different solutions of the solar anomaly.

proposal advanced so far that approaches these aims is LENS [35]. The proposed reaction is the ν_e capture (inverse beta decay) by ^{176}Yb nuclides that go into an excited ^{176}Lu state. The electron resulting from the capture and the delayed γ , used as a tag from the excited Lu decay, are detected as shown in Fig. 33. Notice that the ^{176}Lu ground state is higher than that of ^{176}Yb , making this nuclide stable against beta decay. The stability of the target nucleus is mandatory, otherwise (as for example ^{115}In), its β decay electrons that are not

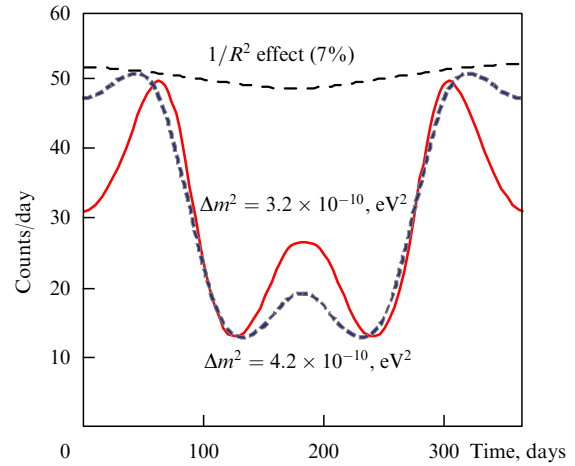


Figure 32. Expected seasonal variations of the counting rate in BOREXINO for two different values of δm^2 and maximum mixing ($\theta_{12} = \pi/4$) compared with the purely geometrical effect due to the eccentricity of earth's orbit.

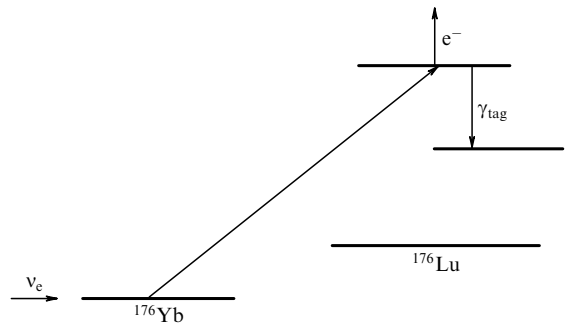


Figure 33. Schematics of the energy levels involved in the electron-neutrino capture by ^{176}Yb .

distinguishable from the electrons from the capture (the signal) would give unacceptable background levels.

These characteristics and the low (301 keV) threshold for neutrino capture make ^{176}Yb practically unique.

Capture electrons and tag photons are detected via the scintillation light of a liquid scintillator in which the Yb is doped. A 20 t natural Yb detector will provide a yield of 200 events/year in the pp branch, 280 in the Be branch and 16 in pep if the standard solar model is correct. The presence of the γ tag allows for less stringent radiopurity levels than BOREXINO. Nevertheless, a number of problems must be solved. The techniques needed to prepare large quantities of a scintillator doped with a large fraction of Yb (at least 8%), with a reasonable light yield, good attenuation length (several metres), and chemical stability must be developed. The detector liquid must also be such that it can be safely operated underground without danger the population in case of accident.

The requested radiopurity levels of the scintillator's environment must be obtained. Neutrino sources necessary for calibration must also be procured.

If the ongoing R&D program is to be successful and LENS to be built, its results will be extremely relevant. The expected yield strongly depend on the mixing parameters allow them to be determined accurately. Figure 34 shows the energy spectra as expected in the standard solar model and as modified in the cases of the four main solutions. In the SMA

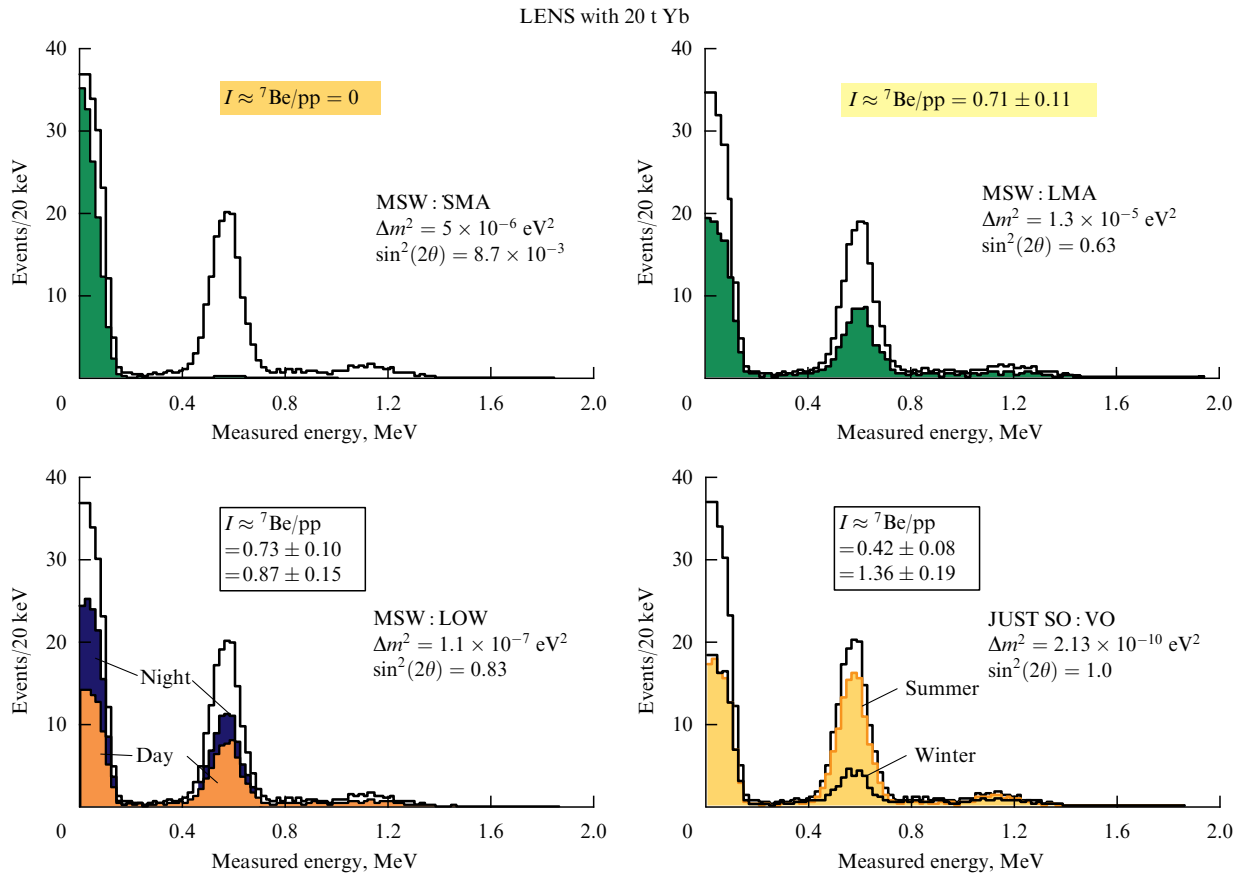


Figure 34. Energy distributions as expected for LENS in different solutions of the solar anomaly. θ is θ_{12} .

solution, the count will be zero for the Be line and almost 100% for the solar model in the pp. In the LMA solution, both in the Be and in the pp regions, the count will be close to 50%. In the LOW, both pp and Be will be suppressed with strong differences between day and night. Finally, in the Just So solution, strong seasonal variations will be observed. Notice also that, with reference to Be, LENS is sensitive to electron neutrinos only, while BOREXINO is sensitive to all the flavours, providing, when taken together, good flavour sensitivity.

11. The search for cold dark matter

Astronomical observations have shown that matter in the universe constitutes much more than what we actually see. We see the stars and other luminous objects because they shine light or other electromagnetic radiation. We can then evaluate the total ‘luminous’ mass, for example, of a galaxy. On the other hand, by measuring the speed of the gas clouds orbiting around the galaxy we can easily infer, with Newton’s law, the total mass of that galaxy. The result is that this total mass is at least ten times the luminous mass. We conclude that the universe contains matter of unknown form and call it generically ‘dark matter’.

There are two possible types of dark matter. The first are heavenly bodies that are too small to shine light (like the planets, for example); in this case the unseen matter is made up of just the normal stuff, of elementary particles, collectively called baryons, and is called baryonic dark matter.

The other possibility is that dark matter is made up of elementary particles interacting only weakly with ordinary

matter, and we have not yet detected them. There may be a contribution of neutrinos, if they have any mass, since we know that the universe is full of neutrinos ($125/\text{cm}^3$ per flavour, the counterpart of the cosmic microwave background). As neutrinos move at relativistic speed, this is called ‘hot’ dark matter. Another even more exciting possibility is the presence of some not yet discovered weakly interacting elementary particles, similar to neutrinos, but much more massive, perhaps hundreds of GeV. These hypothetical particles are collectively called WIMPs (Weakly Interacting Massive Particles). As they are non-relativistic, their contribution to dark matter is called ‘cold’.

We have indeed strong reason to believe that non-baryonic dark matter exists. The evidence comes from the measurement of the primordial abundance of light elements, in particular deuterium, that were synthesized when the universe was young, small, and very hot, with a process that depends on the total baryonic mass. From the measured values of the abundance, we evaluate a total baryonic mass that is much smaller than the total dark matter. Non-baryonic dark matter must exist.

A hint on the nature of non-baryonic dark matter comes from elementary particle physics. The SM has been successfully tested with high precision experiments but we know, mainly on the basis of logical arguments, that it is probably incomplete. Among the best candidates to extend the theory is supersymmetry. This theory assumes that every elementary particle has a companion, called a superpartner. The lightest, presumably the neutralino, is stable. As such, neutralinos produced in the first instants of the universe, should still be present around us. We do not sense them because, like

neutrinos, they interact only very weakly with matter, although neutralinos might account for a large fraction of the mass of our universe.

Neutralinos are being actively searched for at accelerators but have not been found up to now. The results of the LEP experiments, in particular, imply that neutralinos, if they exist, have rather large masses, larger than 50 GeV.

At Gran Sasso, different experiments are taking data or are in different stages of their R&D in the search for dark matter, more specifically for non-baryonic cold dark matter, or WIMPs. These experiments are extremely difficult and delicate.

We assume that our galaxy contains cold dark matter in the form of WIMPs distributed smoothly as an enormous cloud with a density, at our place, of a few GeV/cm^3 . The sun moves in the galaxy at 230 km s^{-1} across the WIMP cloud. The earth moves around the sun at 30 km s^{-1} . In June, its direction is parallel to that of the sun, in December anti-parallel. The WIMPs enter our detector with a velocity v of the order of 230 km s^{-1} ($\beta \approx 10^{-3}$). If a nucleus of mass M is hit, it will recoil with a kinetic energy

$$E_k = \frac{\mu^2}{M} \beta^2 (1 - \cos \theta),$$

where μ is the mass of the WIMP and θ is the scattering angle. For $\mu = \text{GeV} - \text{TeV}$, $E_k = 1 - 100 \text{ keV}$, a very low energy indeed. To make things more difficult, only a fraction Q of the energy released in the detector can be detected. For scintillators examples are $Q = 0.1$ for I, $Q = 0.25$ for Ge, $Q = 0.6$ for Xe, while for bolometers Q is close to 1. Notice also that the energy spectrum of the WIMP signal is a maximum at the lowest energy and decreases rapidly with increasing energy, exactly as the backgrounds do!

The signals from WIMPs are also very rare and heavy nuclei have to be used as targets. Given the large wavelength of the WIMPs, they 'see' the nucleus as a unique object, in other words, they scatter coherently with a probability proportional to A^2 . But even for coherent interactions, the rates are small. For example, supersymmetric models predict rates between 10 and 10^{-6} events per day per kilogram of detecting mass. A low background environment is clearly mandatory. Detectors must have a very low energy threshold, a large sensitive mass (tens to hundreds of kilograms or more), good energy resolution, an ultra high radiopurity, and efficient background discrimination.

The groups active at Gran Sasso have developed three principal world-leading techniques.

The first is based on large mass scintillator media, both crystals and liquids, and has been developed by the DAMA collaboration.

The second technique is based on bolometers at sub-Kelvin temperatures. The CRESST experiment has performed the necessary R&D in recent years and its detectors are now approaching an interesting sensitivity and adequate background levels. The Milan group is also active in this sector in the framework of the MIBETA, CUORICINO, and CUORE experiments.

Finally, the third is based on germanium detectors, used in the search for double beta decay, by the Heidelberg group. World record background rates have already been obtained in this energy region, i.e., around 2 MeV. Research and development is needed to decrease background rates in the very low energy region relevant for dark matter searches, i.e., 10–50 keV.

As a result of the strong R&D program, DAMA has been running for several years a set of NaI (TI) radio-pure crystals with a total mass of 115 kg. The strategy of the experiment is to search for an annual modulation of the counting rate at low energy, a feature characteristic of the signal but not of the background (or at least of the major part of it). As mentioned above, the speed of the earth, and of the detector, with respect to the galaxy, or the WIMPs, varies during the year, with a maximum in June and a minimum in December. Taking into account the fact that the ecliptic is not parallel to the sun's orbit, one finds that the peak to peak speed modulation amplitude is 7%, the maximum expected modulation in the WIMP yield.

Figure 35 shows the DAMA counting rate [36], after subtraction of the constant part, as a function of time over a four-year period. While in the first phases the data collection periods were interleaved with maintenance periods, in the last years the data collection was never interrupted. In the figure I took the liberty to add a sinusoidal curve to show the characteristics of the expected signal.

Assuming that a WIMP signal is indeed observed, the fit performed by the collaboration gives the result shown in Fig. 36, where ξ is the ratio between the actual (unknown)

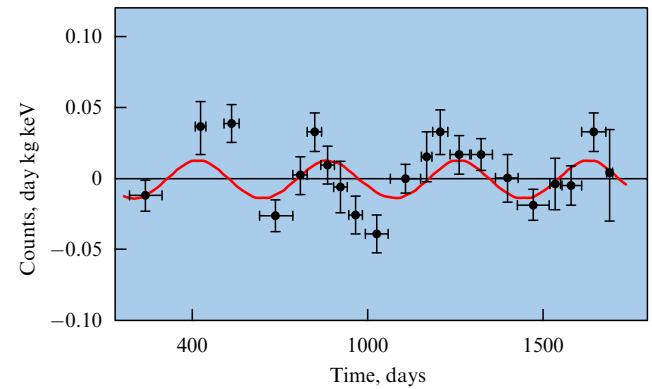


Figure 35. DAMA counting rates after subtraction of the constant term as a function of time. I included a sinusoidal curve to show the expected characteristics of the signal.

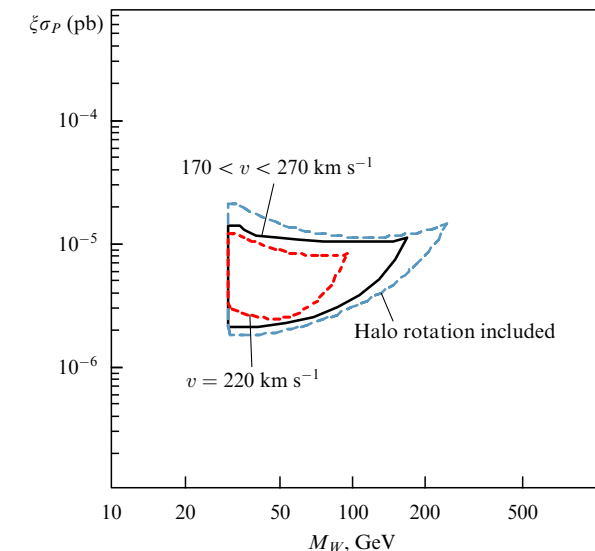


Figure 36. Regions of the parameters space obtained by DAMA in a fit assuming WIMP signal with different characteristics.

and the assumed WIMP density. The different contours represent different assumptions about the WIMP distribution.

These results are extremely interesting but much more work is still needed. The one-year period, for example, is common to many physical phenomena, some of which might contribute to the background, maliciously faking a signal. DAMA has already looked into all conceivable possibilities of this type and has been able to exclude them, but further checks are needed.

While DAMA is still taking data, in its 6th annual cycle, a new phase (dubbed LIBRA set-up) is now starting. Powders of increased radiopurity have already been obtained by DAMA and crystals of NaI will be grown out of them for a total mass of 250 kg (twice that of the first phase). A first preliminary data taking period will take place between the end of 2002 and September 2003. Then the full-fledged 4-year data taking campaign will start.

Given the importance and difficulty of the search for dark matter, the program of the Laboratory must include different approaches employing different techniques and different target nuclei.

The approach of CRESST is based on cryogenic calorimeters. The energy released by the recoiling nucleus in the absorber creates phonons that are thermalized and collected by a thermometer located on the surface of the absorber. The thermometer is made of tungsten operating in the superconducting phase (at 12 mK), close to the transition temperature. In this region the electric resistance is a steeply rising function of the temperature. This, associated with the high specific heat values characteristic of cryogenic temperatures, makes the measurement of the resistance a very sensible way to evaluate the energy deposit. There is a wide range of possible absorber materials and CRESST2 has chosen CaWO_4 for the present phase.

Crucial parameters are the energy resolution and the background. A long R&D program has led to proposing that CRESST2 [37] achieve an energy resolution of 133 eV at 1.5 keV and a background $b = 1 \text{ ev. (kg keV d)}^{-1}$ at 15 keV, mainly due to radioactive contaminants. This is not enough.

There are two main contributions to the radioactive background: the (dominant) contribution of electrons and photons through ionisation and the (smaller) one of neutrons. The latter comes from the energy deposited by recoiling nuclei and is substantially indistinguishable from the signal. On the other hand, while phonon detection provides full sensitivity to photons, electrons, and nuclear recoils, ionisation and scintillation signals are smaller for nuclear recoils and higher for electrons and photons. Profiting from this feature, CRESST2 plans to use simultaneous detection of phonons and scintillation light to discriminate, as schematically shown in Fig. 37.

Figure 38 shows the data obtained with a prototype detector exposed to photons and neutron sources. The two bands are clearly separated allowing discrimination of the two samples with high purity. Based on these results, CRESST2, which has been recently approved, plans for a 10 kg detector mass based on 33 modules of 300 g each of CaWO_4 , with a foreseen rejection power of 99.7%.

Over a three year period the sensitivity shown in Fig. 39 is foreseen [threshold = 15 keV, background before discrimination $b = 1 \text{ ev. (kg keV d)}^{-1}$]. The program foresees the production of modules in 2001 and 2002 and a start of data collection in 2003.

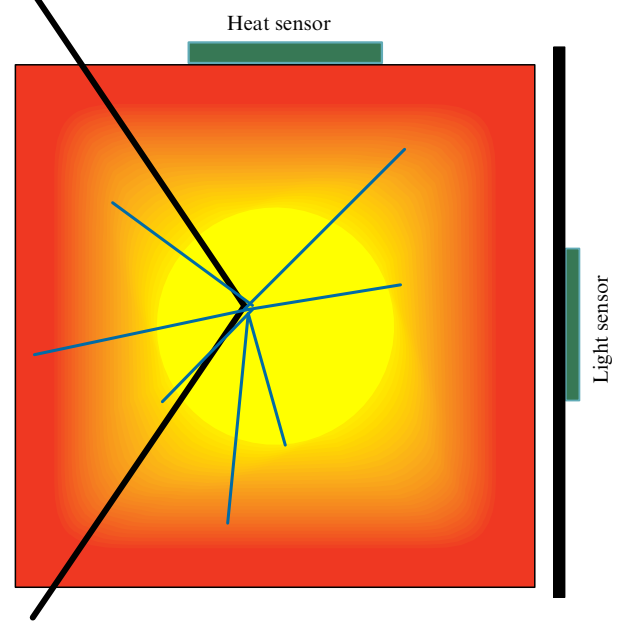


Figure 37. Principle of the CRESST2 detector.

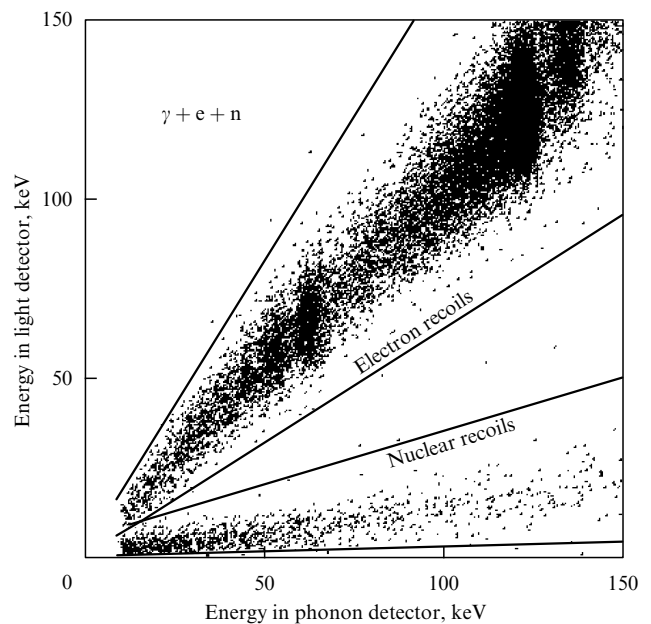


Figure 38. Pulse height in the light detector (keV) vs. pulse height in the phonon detector (keV) in the prototype CRESST2 set-up exposed to an n source and an $e + \gamma$ source.

The third technique in the Gran Sasso program is based on Ge detectors. I have already discussed the Heidelberg–Moscow experiment in the framework of the search for $0\nu 2\beta$ decay. The same apparatus can be used to search for cold dark matter. For this search, the background at 10–50 keV is relevant, a much more difficult region than that of $0\nu 2\beta$ decay (2 MeV).

To decrease the background, the group has proposed the HDMS experiment [38]. It is composed of two detectors: an inner one made of 200 g of (p-type) Ge acting as the sensitive mass and almost completely surrounded by an outer one of (n-type) Ge crystal acting as an anticoincidence to reject the

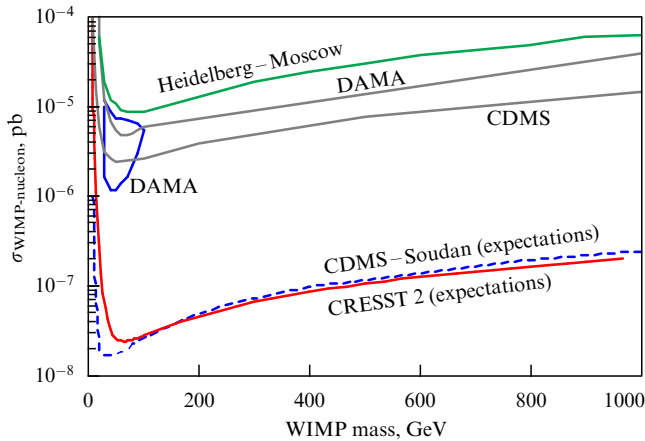


Figure 39. Expected sensitivity of CREST2 for a $10 \text{ kg} \times 3 \text{ years}$ exposure with background before discrimination $b = 1 \text{ ev. (kg keV yr)}^{-1}$. The published best results are included for comparison.

background from the environment (see Fig. 40). A prototype set up has been taking data for more than one year now and has reached in the last period a background level of $b = 0.5 \text{ ev. (kg keV d)}^{-1}$ between 2 keV and 40 keV. An important contribution to the background is given by ^{68}Ge produced by cosmic rays during the growth of the crystals. The final set up, based on enriched ^{73}Ge as the enrichment process eliminates a large fraction of the cosmogenic ^{68}Ge , is now taking data. The projected sensitivity of HDMS extends to cross section values between $2 \times 10^{-6} \text{ pb}$ for WIMP masses of 20 GeV and $3 \times 10^{-6} \text{ pb}$ for WIMP masses of 100 GeV. In particular it will be sensitive in the DAMA region.

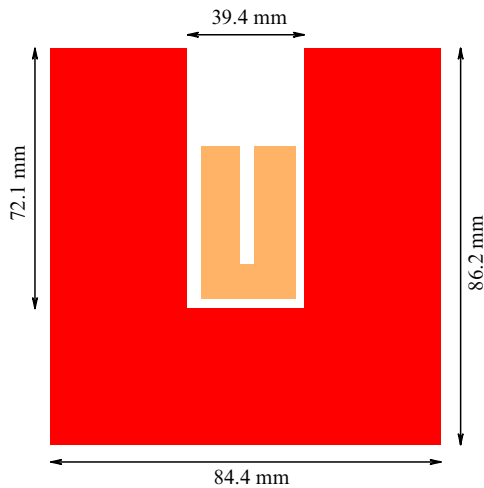


Figure 40. Schematics of the HDMS set-up.

The same group with the GENIUS-TF [10] may obtain similar or better results. This set up has been proposed and approved by the Laboratory mainly as a test facility for GENIUS but can produce interesting results on its own. It uses 14 hyper-pure Ge detectors with a sensitive mass of about 40 kg in a bath of ultra-pure liquid nitrogen surrounded by a number of screens. Monte Carlo calculations show that the background level $b = 10^{-2} \text{ ev. (kg keV d)}^{-1}$ can be reached above 11 keV.

In the longer run, GENINO with its 100 kg mass and GENIUS [9] with its 1000 kg will be able to explore a large fraction of the parameters space. Nevertheless, tremendous efforts will be needed to reduce the background in inverse proportion to the increase in mass.

12. Conclusions

In the last years, a neutrino physics has entered a new age. The discovery of neutrino oscillations has shown that neutrinos have non-zero masses and that leptonic flavour numbers are not conserved. The search for neutrinoless double beta decays has already reached a Majorana mass sensitivity capable of limiting or contradicting some high energy extensions of the SM. Dark matter searches are reaching the area where signals might appear.

These results, which point to physics beyond the standard theory, have been obtained in underground low background laboratories. Gran Sasso has made a contribution, as I have discussed.

An extremely interesting future appears to be in front of us where revolutionary discoveries might become possible. In particular, the space that will be soon available at Gran Sasso, with its high quality infrastructure has stimulated many interesting ideas and proposals. These are in different stages of research and development, and of testing and preparation. Presumably, not all of them will become running experiments, but there is a good chance that at least a few will, with a bit of fortune, produce outstanding results in the coming years.

Acknowledgements

I warmly thank L B Okun, V L Ginzburg, V A Matveev, and O G Ryazhskaya for their kind invitation to deliver the seminars that form the basis for this paper and for helpful discussions. I thank V Berezinski and F Vissani for many clarifying discussions.

References

- Bettini A "The Gran Sasso Laboratory 1979–1999", Preprint INFN (1999)
- Pontecorvo B M *Zh. Eksp. Teor. Fiz.* **33** 549 (1957) [*Sov. Phys. JETP* **6** 429 (1957)]; **34** 247 (1958) [*Sov. Phys. JETP* **7** 172 (1958)]; Gribov N, Pontecorvo B *Phys. Lett. B* **28** 493 (1969)
- Wolfenstein L *Phys. Rev. D* **17** 2369 (1978); **20** 2634 (1979); Mikheev S P, Smirnov A Yu *Yad. Fiz.* **42** 1441 (1985) [*Sov. J. Nucl. Phys.* **42** 913 (1985)]; Mikheev S P, Smirnov A Yu *Nuovo Cimento C* **9** 17 (1986)
- Fogli G L, Lisi E, Scioscia G *Phys. Rev. D* **52** 5334 (1995); Fogli G L, Lisi E, Montanino D *Phys. Rev. D* **54** 2048 (1996)
- Apollonio M et al. (CHOOZ Collab.) *Phys. Lett. B* **466** 415 (1999)
- Vissani F *Nucl. Phys. B Proc. Suppl.* **100** 273 (2001); hep-ph/0012018
- Weinheimer C et al. *Phys. Lett. B* **460** 219 (1999); Neutrino 2000 *Nucl. Phys. B Proc. Suppl.* **91** 273 (2001); Lobashev V M et al. *Phys. Lett. B* **460** 219 (1999); Neutrino 2000 *Nucl. Phys. B Proc. Suppl.* **91** 280 (2001)
- Klapdor-Kleingrothaus H V *Sixty Years of Double Beta Decay — From Nuclear Physics to Beyond Standard Model Particle Physics* (Singapore: World Scientific, 2000)
- Preprints LNGS-LOI 9/97; LNGS-LOI 9/97 add. 1; LNGS P23/2000; GENIUS MPI-Report MPI-H-V26-1999
- Preprints MPI-Report MPI-H-V4-2001; LNGS P27/2001
- Alessandrello A et al. *Phys. Lett. B* **486** 13 (2000)
- Preprints LNGS-LOI 16/99; LNGS-LOI 12/98
- Aglietta M et al. (LVD Collab.) *Nuovo Cimento A* **105** 1793 (1992)
- Fukuda Y et al. (Super-Kamiokande Collab.) *Phys. Rev. Lett.* **81** 1562 (1998); Neutrino 2000 *Nucl. Phys. B* **91** 127 (2001); see [13]

15. Ambrosio M et al. (MACRO Collab.) *Phys. Lett. B* **434** 451 (1998); *Phys. Lett. B* **478** 5 (2000)
16. (MACRO Collab.), Neutrino 2000 *Nucl. Phys. B Proc. Suppl.* **91** 141 (2001)
17. Bahcall J N, Basu S, Pinsonneault M H *Phys. Lett. B* **433** 1 (1998); Bahcall J N, Pinsonneault M H, Basu S *Astrophys. J.* **555** 990 (2001); astro-ph/0010346; Turck-Chièze S, Lopes I *Astrophys. J.* **408** 347 (1993)
18. Cleveland B T et al. *Astrophys. J.* **496** 505 (1998); Davis R *Prog. Part. Nucl. Phys.* **32** 13 (1994)
19. Fukuda Y et al. (Kamiokande Collab.) *Phys. Rev. Lett.* **77** 1683 (1996)
20. Fukuda Y et al. (Super-Kamiokande Collab.) *Phys. Rev. Lett.* **86** 5656 (2001); hep-ex/0103033; Fukuda Y et al. *Phys. Rev. Lett.* **81** 1158 (1998); Erratum **81** 4279 (1998); **82** 1810 (1999); **82** 2430 (1999); Suzuki Y *Nucl. Phys. B* **77** 35 (1999)
21. (GALLEX Collab.) *Phys. Lett. B* **285** 376 (1992); **314** 445 (1993); **327** 377 (1994); **342** 440 (1995); **357** 237 (1995); **388** 384 (1996); **447** 127 (1999)
22. Abdurashitov J N et al. (SAGE Collab.) *Phys. Lett. B* **328** 234 (1994); Abdurashitov J N et al. *Phys. Rev. C* **60** 055801 (1999); Garvin V N, Neutrino 2000 *Nucl. Phys. B Proc. Suppl.* **91** 36 (2001)
23. Altmann M et al. *Phys. Lett. B* **490** 16 (2000)
24. Fogli G L et al. “Solar neutrinos: where are the oscillations?”, in *9th Intern. Workshop on “Neutrino Telescopes”*; Venice, March 6–9 2001; *5th Topical Workshop at the Gran Sasso Laboratory, March 12–14 2001*
25. Bonetti R et al. *Phys. Rev. Lett.* **82** 5205 (1999)
26. (K2K Collab.), Neutrino 2000 *Nucl. Phys. B Proc. Suppl.* **91** 203 (2001)
27. Preprints MINOS Technical Design Report, Nu-MI-L-337, October 1998
28. Preprints CERN 98-02, INFN/AE-98/05; CERN-SL/99-034(DI), INFN/AE-99/05
29. Preprints ICANOE proposal to LNGS-SC and CERN SPSC: LNGS-P21/99, CERN/SPSC 99-25; LNGS-P21/99.Add.1; 2, CERN/SPSC 99-40
30. Rubbia A, Private communication
31. See for example: Richter B, Preprints SLAC-PUB-8587 (Aug. 2000); hep-ph/0008222
32. Preprints CERN/SPSC 2000-028; SPSC/P318; LNGS P25/2000 (July 10, 2000)
33. Preprints LNGS P26/2000; CERN/SPSC 2000-031; SPSC/M657 (August 15th, 2000)
34. Arpesella C et al. BOREXINO proposal (Univ. of Milan) 1991; von Feilitzsch F et al. *Astro Phys.* **8** 141 (1998); Alimonti G et al. (BOREXINO Collab.), hep-ex/0012030 (submitted to *Astropart. Phys.*)
35. Preprints LNGS-LOI 18/99; LNGS P18/99 add.1
36. Bernabei R et al. *Phys. Lett. B* **480** 23 (2000); Bernabei R et al. *Eur. Phys. J. C* **18** 283 (2000)
37. Preprints CRESST2 proposal. LNGS-EXP 29/2001; MPI-PhE/2001-2; LNGS P24/2001 Add.1
38. Preprints HDMS proposal. LNGS-EXP 27/98